Chem Soc Rev

# Dye-Doped Silica Nanoparticles as Luminescent Organized Systems for Nanomedicine



| | |
|---|---|
| Journal: | *Chemical Society Reviews* |
| Manuscript ID: | CS-REV-11-2013-060433.R2 |
| Article Type: | Review Article |
| Date Submitted by the Author: | 17-Feb-2014 |
| Complete List of Authors: | Montalti, Marco; G.Ciamician, Dipartimento di Chimica<br>Prodi, Luca; Universita degli studi di Bologna, Dipartimento di Chimica<br>Rampazzo, Enrico; University of Bologna, Chemistry Dept. 'Ciamician'<br>zaccheroni, Nelsi; University of Bologna, Chemistry Departmetnt 'G. Ciamician' |
| | |

Chem Soc Rev

RSCPublishing

REVIEW ARTICLE

# Dye-Doped Silica Nanoparticles as Luminescent Organized Systems for Nanomedicine

Cite this: DOI: 10.1039/x0xx00000x

M. Montalti,[a] L. Prodi,[a]* E. Rampazzo,[a] and N. Zaccheroni.[a]

Received ooth January 2012,
Accepted ooth January 2012

DOI: 10.1039/x0xx00000x

www.rsc.org/

The ability to find synergic solutions is the core of scientific research and scientific advancement. This is particularly true for medicine, where multimodal imaging and theranostic tools represent the frontier research. Nanotechnology, which by its very nature is multidisciplinary, has opened up the way to the engineering of new organized materials endowed with improved performances. In particular, merging nanoparticles and luminescent signalling can lead to the creation of unique tools for the design of inexpensive, hand-held diagnostic and theranostic kits. In this wide scenario, dye-doped silica nanoparticles constitute very effective nanoplatforms to obtain efficient luminescent, stable, biocompatible and targeted agents for biomedical applications. In this review we discuss the state of the art in the field of luminescent silica-based nanoparticles for medical imaging, starting with an overview of the most common synthetic approaches to these materials. Trying to rationalize the presentation of this extremely multifaceted and complex subject, we have gathered significant examples of systems applied in cancer research, also discussing those that take a multifunctional approach, including theranostic structures. Nanoprobes designed for applications that do not include cancer are a minor part, but interesting achievements have been published and we present a selection of these in a subsequent section. To conclude, we propose a debate on the advantages of creating chemosensors based on luminescent silica nanoparticles. This is far from easy but is a particularly valuable goal in the medical field and therefore subject to extensive research worldwide.

## 1. Introduction

Over the last two centuries, life expectancy has increased steadily, like never before in history,[1] and in addition to improved food and water supply and hygiene, this can be attributed to the great development in modern medicine in both diagnosis and treatment. For further improvements, these complex fields require synergic and multifaceted approaches. For example, modern medical imaging techniques[2] such as magnetic resonance imaging (MRI),[3, 4] computed X-ray tomography (CT),[5] positron emission tomography[6] (PET) and optical imaging[7, 8] allow the diagnosis of many diseases in early stages. However, as each individual method has its pros and cons, synergy can be the only solution to overcome limitations in obtaining comprehensive imaging. Taking this path, multimodal and multifunctional tools combining diagnosis, targeting and therapeutics (referred to as theranostics)[9, 10] represent nowadays the frontier research.

The advent of nanotechnology, which by its very nature is a multidisciplinary field, has opened up the way to merge different types of scientific knowledge to obtain these new materials, with potential that we are, as yet, unable to completely foresee.[11] In particular, merging nanotechnology and luminescent signalling can lead to the creation of unique tools[12] that could lead to great improvements in the technical development of many areas. Photochemistry, which deals with the fundamental interaction of light with matter, has been extensively exploited in the development of supramolecular architectures,[13, 14] capable of coupling elementary processes (light absorption and emission, energy[15] and electron transfer) to obtain more complex functions (directional excitation energy migration or multi electron photo injection). These functional photochemical devices should preferably be self-assembled, a feature of great importance as discussed in a masterly paper by professor J. M. Lehn.[16] He showed chemistry as the bridging science between physics (dealing with the laws of the Universe) and biology (dealing with the rules of life), and self-organization as the driving force behind the evolution of complex matter. Nanotechnology in this scheme could be seen as the bridgehead where the different sciences merge.

Among the immense variety of new materials that nanotechnology has proposed in recent decades, nanoparticles are doubtless those that are most versatile and exploited. In analogy to supramolecular photochemical devices, these nanostructures[17-22] have been implemented by exploiting self-

organizing synthetic strategies that require a non-demanding synthetic effort, but which yield complex materials capable of performing elaborate functions. The systems designed to collect molecular level information about biologically relevant processes through luminescence-related techniques[23-26] have further enhanced the characteristics of luminescence which, by its very nature is a very sensitive technique (down to single molecule detection) offering submicron visualization and sub millisecond temporal resolution. At the same time, many of the typical limitations of conventional luminophores (organic dyes), such as poor photostability, low quantum yield, and aggregation in physiological conditions, have been overcome. Nanotechnology has, in fact, been successfully exploited to design platforms taking advantage of several classes of nanoparticles (organic, inorganic and metallic), which are currently employed as fluorescent emitters, each presenting its own merits and disadvantages. In particular, luminescent dye-doped latex nanoparticles[27, 28] or intrinsically luminescent nanomaterials,[29] such as quantum dots (QDs) are extensively studied.[30-39] Nevertheless, in our opinion, dye-doped silica nanoparticles (DDSNs) are a very successful example, capable of offering all the required features to obtain very effective tools for diagnostic and theranostic applications.[12, 18, 26, 40-44] Their synthetic versatility, in fact, allows the preparation of multifunctional targeted nanosystems (Fig. 1).

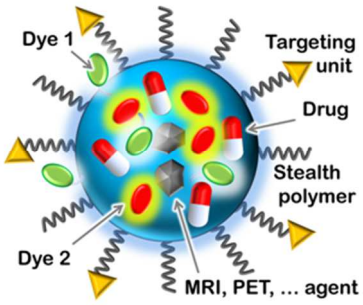


**Fig. 1** Schematic representation of a multifunctional system for nanomedicine.

This is very important to limit the degree of nonspecific interactions and to enhance specific binding by the target sites or internalization by cells that overexpress the target receptors.[2, 45-48] A proper and fine control of functionalization can also yield long-life systems in which the nanoparticle head-off by the RES (Reticulo-Endothelial System) is delayed.

Extensive literature describes the advantages of DDSNs due to their convenient use as fluorescent probes for applications ranging from biosensors[49, 50] to interfacial interaction studies such as immunoassays,[51] multiplexed nucleic acid analysis[52, 53] and drug delivery, to name but a few. The synthetic methods used to prepare DDSNs are all characterized by simplicity, low costs and very slight concerns about their disposal, all features that are obviously desirable if the product is intended to be marketed. Furthermore, these synthetic strategies are characterized by versatility and great control over the architecture of the resulting materials, fundamental points when designing complex systems capable of performing specific functions. For example, the possibility to realize onion-like multilayer structures consisting of a core and as many layers as desired (one or more of these parts could be made of a different material), opens up the way for the design of dedicated multifunctional materials. Moreover, materials prepared for diagnosis and/or therapeutics must be (photo)chemically stable, biocompatible, and non-toxic, all of which are typical characteristics of DDSNs.

To look at the valuable features presented by luminescent silica nanoparticles in a little more detail, one should start from the intrinsic properties of silica, which is photophysically inert (transparent to visible light), with the photophysical properties of the final materials being conferred by the doping and/or the capping agents. Each silica nanoparticle can contain a large number of photochemically active species and consequently present extremely high extinction coefficients, its total value being equal to the sum of those the individual chromophores. Moreover, the silica matrix protects the active species segregated inside the nanoparticle from the chemicals contained in the environment, decreasing the incidence of undesired photoreactions and thus increasing the photostability of the system. Inclusion in this kind of matrix also helps provide the active species with an almost constant environment in chemical terms.

Also the emission properties of luminescent silica nanoparticles are conferred by the doping species and they depend not only on their own characteristics, but also on their possible cross-interactions. Classic photophysical techniques such as steady-state and time-resolved fluorescence and fluorescence anisotropy can provide information on the rotational mobility of photoactive dyes, on the distance and communication between them, and on the effect of signal amplification, as the presence of numerous fluorophores in close proximity can give rise to cross-talking. In DDSNs, homo-energy transfer processes are very important, as they can lead to undesired self-quenching phenomena. However they can also help to obtain directional energy transfer increasing, for example, the signal amplification effect.[54] In DDSNs loaded with different dyes, hetero-energy transfer processes can occur and, with a proper design, they can be intentionally avoided, to obtain ratiometric systems[55, 56] for example, or favoured to optimize internal FRET in order to yield high fluorescence intensity, large Stokes shift and wide absorption with multiple emission colours for applications such as multiplex FRET bioassays.[15, 57]

As a last very important characteristic of DDSNs, we would like to stress that silica does not present inherent toxicity and it does not undergo microbial attack. Toxicity is nevertheless a very crucial point due to valid safety concerns about the potential risks, for both humans and environment, of nanomaterials. Research is actively heading in this direction to assess dangers related to the production and use of silica nanostructures.[58] Key points under investigation are the uptake, transformation, transportation and persistence of nanoparticles. In spite of considerable interest in the biomedical applications of such nanomaterials, human clinical trials are still rare and

this delay is due to the fact that the understanding of their *in vivo* biocompatibility, toxicity and biodistribution remains limited. Only very few nanomedicine-based drug/dye delivery systems have already been marketed. Others are undergoing clinical trial but most still remain in the preclinical development stage. Within this framework, it is now clear why widespread research is trying to provide exhaustive answers to these problems, despite the large number of parameters to be considered. Different design, target environment and dimensions - each with its own surface chemistry[42] - could result, in fact, in a potential different toxicity, and for this reason an accurate characterization of the NPs (including their molar concentration, a parameter that is often not reported) is the appropriate starting point prior to the toxicity assessment.[59] Toxicity is preferentially tested with *in vitro* assays[60, 61] because they are low cost, easy and efficient, while complete *in vivo* test,[62-64] that would include the study of long-term effects, tissue localization, retention and excretion, [42, 65, 66 24, 67]are much more rarely reported. Toxicity, however, depends on the specific particle and on the biological target and therefore rationalization in general behaviour is very difficult and still far from being addressed. Despite the fundamental importance of this branch of research and its fascination, its deep dissertation is beyond the aim of this review. However, readers who are interested can find an increasing amount of specific literature.[68, 69] We can, however, say that the evidence obtained so far points towards the benign nature of DDSNs, when properly designed, and this has greatly stimulated research into more and more complex and multifunctional systems, particular into theranostic and personalized medicinal applications. While personalized disease treatments, based on the molecular profile of each individual patient, are still in their infancy (although they are rapidly developing),[70, 71] research on nanomaterials for theranostic applications is at such a stage that its clinical development is expected to explode in the future. In particular, mesoporous silica nanoparticles are extensively studied as drug delivery platforms for their drug load potential and their flexibility in combination with one or more imaging modes.[72-75]

Up to now we have repeatedly presented the versatility of DDSNs as the main root of their scientific appeal and promising development. At this stage, it is very important to mention that this feature is also due to the inherent characteristics of luminescence spectroscopy. The sensitivity of this technique is universally acknowledged but, in our opinion, its versatility is generally underestimated. It is worth noting that not only can all luminescence parameters such as Stokes shift, intensity and anisotropy, emission and excitation spectra, and excited state lifetime be used for monitoring the target species,[13] but that another equally important element of versatility is related to the different possible origins of the luminescence process itself. In particular, the possibility to generate luminescence in dark conditions - without photo-excitation - allows higher sensitivity through enhancement of the signal-to-noise ratio. The most commonly exploited techniques are chemiluminescence (CL) and electro-chemiluminescence (ECL), namely the luminescence arising from an excited state generated in an electrode by a chemical reaction. ECL, to cite an example, is routinely used for the quantification of biomolecules, with a market that is worth billions of dollars every year. Interestingly, the use of ECL has been also extended to ultrasensitive low-light microscope imaging[19] and ECL nanoprobes are quickly increasing in number and complexity.[21, 22]

We would also like to mention the highly interesting possibilities offered by thermochemiluminescence (TL, in which the excited state is generated by the thermolysis of suitable molecules), which has seldom been explored yet and which has only very recently been used, for the first time, in a convenient temperature range (under 100°C), in combination with silica nanoparticles yielding excellent analytical features.[20] It has to be stressed that the combination of the various luminescence techniques in suitable platforms could make it possible to design ultrasensitive materials for multiplexed experiments both *in vitro* and *in vivo*, and this approach is still unexplored.

In this review article we discuss the state of the art in the field of luminescent (dye-doped) silica-based NPs for medical imaging, starting with a quite exhaustive overview that highlights the main pros and cons of common synthetic approaches to these materials. Trying to rationalize the presentation of this subject, which is highly multifaceted and complex, we have gathered significant examples of systems aimed at application in cancer research, also discussing those that take a multifunctional approach, including theranostic structures. Nanoprobes designed for applications that do not include cancer are a minor part, but some very interesting achievements have been presented and we have dedicated a section to a selection of them. To conclude, we propose a brief discussion on the advantages of creating chemosensors based on luminescent silica nanoparticles, a far from easy but particularly valuable goal in the medical field and therefore subject to extensive research worldwide.

## 2. Synthesis of luminescent silica nanoparticles

The synthesis of silica nanoparticles in solution can be obtained with sol-gel processes[76] in various conditions that lead to different final materials by tuning parameters such as catalytic conditions and nanoparticle nucleation-growth confinement. All these synthetic strategies, however, usually share tetraethoxysilane (TEOS) as their silica precursor and characteristics such as simplicity, low costs, versatility and control over nanoparticle dimensions. The main synthetic approaches are the Stöber-Van Blaaderen method and those involving hydrolysis and condensation confinement, known as reverse microemulsions (water-in-oil)[77, 78] and direct micelles assisted methods (Fig. 2).[78-80] Each synthetic approach presents advantages and limitations that are transferred to the resulting nanostructures, designed to suit particular applications.

As a general indication, the use of trialkoxysilane derivatized dyes[81, 82] ensures condensation of the fluorophores within the silica matrix, preventing the leaching of dye from the particles.

This is closely related to the sensitivity (signal-to-noise ratio) of the system and it is particularly relevant with NPs with a high surface-to-volume ratio. In biological applications, the release of hydrophobic dyes, even when not observed in pure water, can be promoted by the presence of proteins and a lipophilic cellular microenvironment.

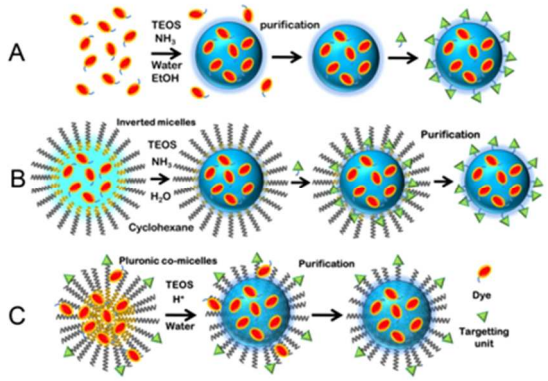


**Fig. 2** Schematic representation of different synthetic strategies to obtain dye-doped silica nanoparticles: Stöber method (A), reverse microemulsion method (B) and direct micelles assisted method (C). Adapted from ref. [12] Copyright 2011 Wiley Publishers Ltd.: *Angew. Chem., Int. Ed.*.

The number of molecular dyes that can be used for NPs doping is usually quite high but it depends on the synthetic strategy adopted. Limitations are mainly related to solubility in the reaction milieu and to the synthetic accessibility of the trialkoxysilane derivatives. Another important point is the electrostatic interaction between the dye and the silica matrix which generally favours the inclusion of positively charged dye and hampers negatively charged species.

In the case of diagnostic applications, the combination of several factors linked to the brightness of the system, to spatial control over nanoparticle functionalization and to the colloidal stability of the NPs suspension, determines the suitability of the synthetic method.

### 2.1 Stöber method

The pristine study of Kolbe,[83] successively developed by Stöber,[84] to obtain colloidal silica was later implemented by Van Blaaderen to obtain fluorescent NPs, thanks to the incorporation of trialkoxysilane modified dyes (fluorescein in his first report).[85] This method is far from dated, thanks to an accessible dimensional range spanning from 10 to several hundreds of nanometres (with one-pot procedures), very simple synthetic mixtures (TEOS, water and ammonia), mild conditions and the possibility to obtain very monodisperse NPs. In this strategy, TEOS hydrolysis and NPs formation is promoted by ammonia and water using ethanol as TEOS co-solvent. The NPs dimension can be controlled by varying the concentrations and ratios of the components. Covalent doping of the NPs is achieved by using alkoxysilane derivatized dyes, with some limitations due to their solubility in ethanol-water mixtures. The luminescence properties of these systems depend on the mutual position of the condensed fluorophores within the NP. This aspect has been investigated by only a few research groups using quite different approaches[11] that have demonstrated how self-compartmentalization of the dyes occurs during NP formation and leads spontaneously to core-shell structures.[86] Two different interesting variations on this approach have been proposed: the use of a biphasic reaction medium or of dye-rich cores as nucleation seeds. The biphasic strategy (water-hydrocarbon) employs a phase transfer approach to modulate the TEOS precursor supply into the medium where the NPs are growing[87] and amino acids as hydrolytic catalysts. This strategy enables to obtain very small nanoparticles (diameters of around 10 nm) and to develop multiple-shell nanoparticles, thanks to the fine control over the hydrolysis and condensation steps that prevents unwanted processes such as parasite nucleation leading to polydispersity and aggregation.

The second method, developed by Wiesner and co-workers, consists of a heterogeneous nucleation[88] with dye-rich cores acting as seeds, that are subsequently covered by a denser silica network.[89, 90] These fluorescent silica NPs (*Cornell* Dots also called *C*-Dots) have a core-shell structure that efficiently shields the dyes from solvent interactions which can be detrimental to photostability and improves the control over NPs dimensions and monodispersity. These last parameters are very important since they are closely linked to the clearance behaviour of NPs *in vivo*.[67]

In the Stöber-derived strategies, the presence of deprotonated Si-OH groups on the surface of the NPs usually generates colloidal suspensions that are strongly stabilized by electrostatic repulsion and are characterized by very large negative ζ-potential values. NPs functionalization exploits the presence of the Si-OH groups and is usually carried out in solution, adding alkoxysilane components tailored for different applications. This second step is quite delicate since it often induces aggregation or leads to incomplete surface passivation.

Purification steps are usually the final part of almost all NPs synthetic protocols and are necessary to separate uncondensed dyes, oligomers and condensation catalysts, and to change suspending media when necessary. These strategies may include precipitation-centrifugation, ultrafiltration (UF), size exclusion chromatography (SEC), dialysis or instrumental techniques such as Flow Field Flow Fractionation (FIFFF).[91] These last three purification methods involve very mild conditions and consequently stand out for the prevention of NPs aggregation.

### 2.2 Reverse microemulsion method

An appropriate mixture of a surfactant and a hydrocarbon induces the formation of a dispersion of reverse micelles, capable of housing a finite amount of water forming a macroscopically isotropic reverse microemulsion (water-in-oil), with water cores that can be exploited as nano-containers to confine the Stöber synthetic process. Several protocols of this kind have been proposed to give quite simple access to nanoparticle preparation and surface modification in the dimensional range of circa 15-200 nm,[78, 92] where the

 

dimension depends largely upon the surfactant type and the surfactant-to-water molar ratio.[93] This synthetic approach is usually appropriate for positively charged water soluble dyes,[77, 94, 95] since they can be easily incorporated into the reverse microemulsion water cores and retained within the nanoparticle silica matrix by electrostatic interactions. This prerequisite constitutes a very strong limitation for the synthesis of fluorescent nanoparticles doped with water insoluble fluorophores or negatively charged ones. On the other hand, this strategy stands out in preparing multiple-layer silica structures and it is also a very suitable and versatile method to cover NPs of others materials (metals, QDs, iron oxides, etc.) with a silica shell, since the presence of the microemulsion prevents aggregation and parasite nucleation during the addition of the components. As silica condensation takes place, with the diffusion of TEOS and other reagents toward the interface of the microemulsion water cores,[96] the same synthetic scheme offers the possibility to introduce chemical functionalities for colloidal stabilization or targeting. Some evidence suggests that this last step can be achieved more efficiently by adding the appropriate silane derivative together with small amounts of TEOS.[78, 92] Final purification steps are always needed to separate the nanoparticles from the large amounts of surfactant and organic solvent that constitute the reverse microemulsion. The main drawback of the reverse microemulsion approach is that these work-up procedures usually involve concentration-dispersion steps that can lead to irreversible aggregation.

### 2.3 Direct micelles assisted methods

In a parallel way, surfactant aggregates or co-aggregates form micelles in water that can be used as self-organized templates to confine the growth of the silica nanoparticles. This is possible because of the lipophilic nature of silica precursors such as TEOS or other organo-alkoxysilane; a large range of organic dyes can be used as doping molecules with this approach. The general strategy involves a water solution of a low molecular weight surfactant (sometimes together with a co-surfactant) and a condensation process driven by ammonia that leads to monodisperse nanoparticles with a diameter from 5 to about 90 nm, a range that is particularly suitable for *in vivo* and *in vitro* applications. After the formation of the nanoparticles, the colloidal suspension usually undergoes purification (dialysis, UF, centrifugation) to remove surfactants, silica oligomers and non-trapped dyes.

Due to the organo-silicate nature of the core, these nanoparticles are often called ORMOSIL (ORganic - MOdified - SILica) and Prasad and coworkers have made the majority of the contributions in the field, proposing many systems within the 20-30 nm range diameter obtained from oil-in-water systems made up of DMSO, water, 1-butanol and surfactant. Low molecular weight surfactants such as AOT (Bis(2-ethylhexyl) sulfosuccinate sodium salt) or Tween 80, are frequently used, while the hydrolysis of the lipophilic silica precursor VTES (triethoxyvinylsilane) is promoted by the addition of APTES (3-aminopropyltriethoxysilane) or ammonia.

The presence of the surfactant and the low reticulation deriving from the trialkoxysilane precursors lead to some mesoporosity so that doping moieties such as dyes[97] and PDT agents[98-100] usually need to be covalently linked to the nanoparticle to prevent leaching.[101, 102] Another important consequence of the relatively high mesoporosity of the NPs obtained with this method is higher oxygen permeation which, on one hand, can lead to lower luminescence intensity, while, on the other hand, it can make the PDT process more efficient, as it will be discussed later on. Targeting and labelling capabilities are readily accessible through nanoparticle functionalization, with groups such as -$NH_2$, -COOH, -SH that allow for conjugation with bioactive molecules (Fig. 3).[43, 103, 104]

Colloidal stability and non-adhesion properties toward proteins can be improved by polyethylene glycol (PEG) derivatization,[105] while the incorporation of QDs[106] and $Fe_3O_4$ nanoparticles[107] can yield hybrid multimodal systems. These features make ORMOSIL nanoparticles very versatile structures for the development of theranostic nanoprobes.

Dealing with DDSNs, to obtain a satisfactory balance between brightness and dimensions is not an easy task as they tend to be mutually exclusive. In this context we would like to mention the recent contribution of Wiesner and co-workers to the development of tiny silica nanostructures preparing sub 10 nm mesoporous PEGylated nanoparticles in the presence of hexadecyltrimethylammonium bromide (CTAB) micelles (Fig. 4).[108]

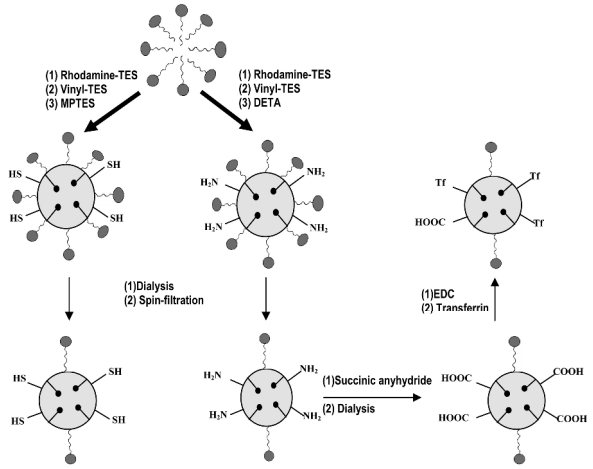


**Fig. 3** Schematized synthesis for rhodamine-doped functionalized ORMOSIL nanoparticles. Reprinted with permission from ref. [43]. Copyright 2008 American Chemical Society.

They were moved by the need to obtain very small targeting agents with improved biodistribution and renal clearance capabilities. They succeeded in synthesizing mesoporous silica nanoparticles (called mC-Dots) ranging from 6 to 15 nm with increments below 1 nm, taking advantage of the rapid hydrolysis of a different silica precursor (TMOS, tetramethylorthosilicate), slow condensation processes and

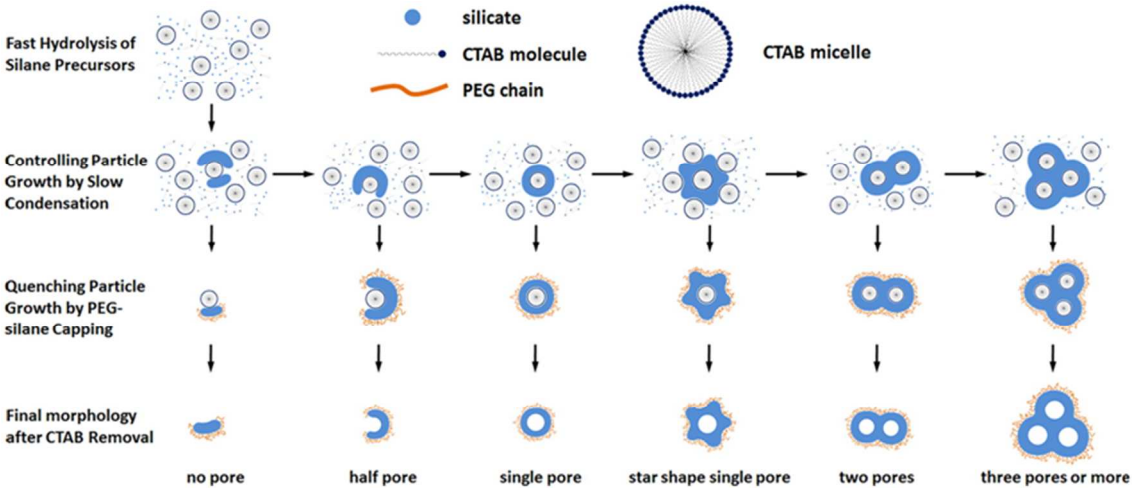


**Fig. 4** Schematization of the synthesis procedure of ultrasmall mesoporous silica nanoparticles. Dependence of the different particle size and morphology from the growing time and quenching conditions. Reprinted with permission from ref. [108]. Copyright 2013 American Chemical Society.

stopping particle growth by adding a PEG-alkoxysilane at different times during synthesis. This capping strategy also affected the nanoparticle morphology, which was found to depend on the average number of micellar aggregates trapped in each nanoparticle core during the condensation process (Fig. 4). They also generalized the first results on NIR emitting sub 10 nm nanoparticles doped with Cy5.5 fluorophores[109] using other fluorophores, such as DEAC and TMR, obtaining blue and red emitting mC-Dots respectively. Thanks to their small dimensions, the renal excretion of these nanoparticles was proved *in vivo*.

A different synthetic possibility is to use a direct micelle assisted strategy with high molecular weight surfactants. Several groups have exploited the template effect of surfactants such as Pluronic F127, F108, or Brij700 to synthesize silica cross-linked micellar nanoparticles featuring core-shell structures,[79, 110, 111] or to obtain size-tunable properties in the presence of an organic swelling agent (trimethylbenzene).[112] This last approach has also been extended to the development of small (d < 25 nm) hollow organosilica nanospheres using bridging organo-silane precursors and Pluronic F127.[113] In another similar example a judicious choice of dialkoxysilanes, swelling agents and surfactants have yielded to the synthesis of both hollow silica nanospheres and organosilica nanotubes.[114] In most cases, these synthetic protocols present condensation processes that are promoted in an acidic environment, using acids such as HCl[110, 113] or HOAc,[115] a set of conditions (pH < 4) in which hydrolysis has faster kinetics with respect to the condensation rate and that stimulates the formation of Si-O-Si chains in the early stages of polymerization,[116] which finally undergo cross-linking.[117] This excludes the nucleation and growth of silica nanoparticles typical of the Stöber process under basic conditions and it enables the confinement of the silica matrix exclusively in the micellar environment, together with the entrapment-adsorption of these surfactants to the silica core, with the valuable consequence of nanoparticle surface modification in a single procedure. From this point of view the Pluronic F127 (MW 12.6 KDa), with its tri-block PEG-PPO-PEG (poly(ethyle glycol)-poly(propylene oxide)-poly(ethylene glycol)) structure and quite large micellar aggregates in water (hydrodynamic diameter ~ 22-25 nm),[118] is, up to now, probably the most versatile surfactant for this kind of application. The relatively polar PPO inner core[118] of these aggregates enables to use TEOS as silica precursor instead of more lipophilic organo-alkoxysilanes, contributing to the formation of a more stable and dense silica network, in which many kinds of alkoxysilane derivatized dyes, from polar to very lipophilic, can be used as doping units. All these features sum with a one-pot mild condition synthesis that yields to PEGylated nanoparticles endowed with very high monodispersity, colloidal stability and core-shell structure. A leading part in the development of fluorescent nanoparticles obtained by Pluronic F127 micelles assisted method was played by our group.[12] These nanoparticles were recently reported with the acronym PluS NPs (Pluronic Silica NanoParticles)[119] and we exploited the versatility of these systems in several fields spanning from photophysical studies,[17, 119] sensors,[41, 120] imaging,[115] fluorescent-photoswitchable nanoparticles,[121] and ECL.[21, 79] From a morphological point of view, these NPs had a silica core of about 10 nm, and an overall hydrodynamic diameter of about 25 nm.

The core-shell structure was verified using several experimental techniques, such as TEM and DLS (Dynamic Light Scattering),[17] AFM measurements[79] and $^{1}$H-NMR and TGA (Thermo Gravimetric Analysis), which respectively showed the outward orientation of the PEG chains and an invariant mass ratio between the organic and inorganic parts of samples

subjected to ultrafiltration treatments of different duration (membrane cut-off 100 kDa).[21]

In these nanostructures the functionalization, for labelling[46] or non-specific targeting,[65] was efficiently obtained with the pristine modification of the Pluronic F127 hydroxy end groups without affecting the one-pot nature of the synthetic method. We found that cellular uptake was influenced by nanoparticle functionalization and PluS NPs cytotoxicity was negligible for nanoparticles with an external PEG shell or presenting external amino- or carboxy-groups toward several normal or cancer cell types, grown either in suspension or in adherence.[65] Very recently, the mesoporous nature of PluS NPs[122] was exploited to tune their charge properties to obtain a programmed charge positioning scheme to influence their biodistribution in targeting applications such as NIR regional lymph node mapping.[42]

### 2.4 Nanoparticles functionalization

In this paragraph, we would like to highlight some relevant issues related to DDSNPs surface modification, via both adsorption processes and covalent couplings. A comprehensive overview of the strategies leading to NPs-biomolecules conjugates is however beyond the scope of this review, since this topic has been covered very recently.[123] Beside the vast and exhaustive review by Igor L. Medintz and co-workers,[123] there are other more focused examples dealing with chemistry bioorthogonality,[124] different kinds of biomolecules (aptamers,[125, 126] proteins[127]) or nanoparticles (inorganic NPs,[128, 129] QDs,[130-132] dye doped polymer NPs,[133] silica coated NPs,[134] or silica NPs[135-138]).

The possibility to display proper functional groups and biomolecules on NPs is a fundamental tool in nanomedicine, since this can allow to exploit the nanoparticle properties at the biological level. This approach defines the "nano-bio interface", determining the response of the biological environment to the NP. Usually, proteins immediately cover any colloidal synthetic material by a process governed by non-covalent adsorption interactions. The mono- or multilayers formed in this way around the NP are called "protein corona",[139, 140] and largely contribute to define the colloidal stability, together with nanomaterials toxicity and clearance.[141, 142] The action of the reticulo-endothelial system (RES), is for example mediated by macrophages (mainly Kupffer cells of the liver) that recognize specific proteins on NPs surface rather than the NP itself.

Up to now the understanding of NPs interactions within living systems is more than a step behind the large achievements obtained in the synthesis of nanomaterials. This is a serious gap to achieve a safe design of NPs for specific biomedical applications. This situation is also complicated by the different response that every kind of cell has toward nanomaterials, an entangled situation for which the concept of cell "vision" was introduced.[141]

In general a non-covalent functionalization strategy of NPs, based on adsorption or electrostatic interactions, can be applied to large molecules such as proteins or polymers. The amphipathic nature of proteins allows for their nonspecific interactions with the NP surface,[143] interactions that are mutually influenced by NPs curvature and protein molecular weight.[144] This approach was also used with silica coated magnetic NPs,[145] and in principle does not require a pristine surface modification since it is governed by the affinity constant of the protein toward the NP surface. Adsorption may lead to protein conformational change and also to denaturation, especially in the case of macromolecules having a low internal stability. [146, 147]

On the other side, a rational way to exploit non-covalent electrostatic interaction is the Layer-by-Layer strategy (LbL),[143, 148, 149] that takes advantage of the development of alternating layers of cationic and anionic electrolytes such as poly(ethyleneimine), poly(lysine), poly(allylamine), poly-carboxylic and poly-sulfonic acid etc., on the NPs surface to mediate the interaction with charged biomolecules. For example, silica NPs passivated with poly(ethyleneimine) and poly(lysine) were loaded with oligonucleotides, to develop nonviral DNA transfection agents.[150, 151]

Besides adsorption and electrostatic interactions, covalent coupling provides a stronger link between the NP and a selected biomolecule, obtaining more robust conjugates, that are less influenced by external conditions, such as protein concentration, pH and ionic strength. In the whole set of NP constituent materials, silica is – remarkably – one of the few that is suitable to direct functionalization. This process is usually exploited through the formation of robust siloxane bonds, using the well established siloxane chemistry.[152] The versatility offered by this chemistry, together with the intrinsic hydrophilic and biocompatible properties of silica, have spread the use of this matrix also as coating layer for other NPs more difficult to functionalize.[134, 153-155] The functionalization of the silica NP surface sites is favoured by the presence of a large library of commercially available chlorosilane and alkoxysilane, that allow to introduce chemical functionalities such as amines,[43, 104, 156, 157] carboxylates,[158] epoxides[159, 160] and thiols.[161-163]

In some examples developed by our research group, core-shell silica NPs obtained with a direct micelles strategy based on Pluronic F127 surfactant were endowed with chemical functionalities (-COOH, -$NH_2$) coming from the pristine functionalization of the Pluronic F127 hydroxylic tips. This approach - with a one-pot procedure - provides NPs with a PEG shell and the desired functional groups, eliminating any need of post-functionalization processes. Moreover, it allows to improve the control over the total number of chemical functionalities per particle, to obtain NP-oligopeptide conjugates,[164] efficient cell internalization,[65] or to accurately tune the NP ζ-Potential for sentinel lymph node mapping.[42]

The majority of the coupling strategies applied to NPs are still deeply-rooted on standard bioconjugation techniques involving -$NH_2$/-COOH groups, a kind of chemistry developed for the radio- and fluorescent labelling of proteins, enzymes and antibodies.[165, 166] This strategy is also well suited for coupling processes involving biomolecules such as oligopeptides or

small aptamers. In these cases the conjugation yield can be maximized using an appropriate excess of coupling reagent, such as carbodiimides (EDC, 1-ethyl-3-(3-dimethylaminopropyl)carbodiimide), since each biomolecule has just few reactive groups and the purification of the NP-conjugate can be easily achieved by means of standard techniques such as size exclusion chromatography (SEC), ion exchange chromatography, dialysis or ultrafiltration.

In the last years more complex coupling processes have boosted the importance of the bio-orthogonality concept in bio-conjugation chemistry.[124] Quite often, in fact, the standard carbodiimide approach is characterized by poor results, especially when the coupling process involves systems having comparable dimensions, and presenting a high density of functional groups. In these cases the overactivation process - carried out in buffered aqueous conditions to limit the hydrolysis of labile o-acylisourea intermediates - frequently brings to a decrease of the colloidal stability and to parasite processes such as omocoupling (protein-protein and NP-NP cross-linking) and poor control over biomolecule stoichiometry and/or orientation. Moreover, the use of an excess of the biomolecules to enhance the coupling yield is often not possible due to their limited availability, and the purification of the bioconjugates can be very difficult in systems where the size of the partners are very similar. For these reasons it is often convenient to apply coupling strategies dealing with less labile intermediates such as thiol-maleimide, also because the concentration of thiol groups in proteins is limited in comparison to $-NH_2$ or -COOH.

More recently, coupling strategies based on click chemistry reactions were also proposed,[167] such as CuAAC (Copper catalyzed Azide-Alkyne reaction),[168-170] hydrazone and oxime ligation. They will surely become more frequent in NPs-bioconjugation protocols, as proved by the increasing commercial availability of tailored etherobifunctional cross-linking reagents.

It is also worth to mention another emerging strategy in the field of conjugation chemistry that is the enzyme-catalyzed bioconjugation. Only few examples of this approach are reported in the field of NPs-bioconjugation, and are related to the derivatization of QDs, virus particles and SPION; we are however confident that it will have an important influence also on silica NPs in the next future. In this context, the more promising approaches are probably the use of Biotin Ligase,[171, 172] Intein-mediated protein ligation[173, 174] and enzymatic self-Labeling (Halo-Tag).[175, 176]

## 3. Silica nanoparticles in cancer research

### 3.1 NPs for optical imaging

Many groups are exploring, in their research activity, core-shell silica nanoparticles obtained for example by stabilizing micelles into silica-like nanoparticles to prepare more robust systems. Subsequently, using the direct micelles assisted method we developed several luminescent nanoparticles based on aggregates of Pluronic F127 surfactant or co-aggregate of F127 and derivatized F127 as templates (Plus NPs). This synthetic method provides nanoparticles with outstanding colloidal stability and well-defined morphological properties that make them ideal candidates for *in vivo* and *in vitro* applications. Their PEG shell and small dimensions (25 nm hydrodynamic diameter), in particular, endow them with improved non-adhesive properties in the presence of proteins, also compared to commercial hydrophilic QDs, with the consequence of ensuring more dynamic behaviour and long circulation times *in vivo*.[115]

Aiming precisely at this kind of application, we realized NIR emitting nanoparticles doped with a Cy7 heptamethine dye, alone or together with a trialkoxysilane derivative of rhodamine B, as suitable probes for optical imaging and as a possible alternative to commercially available fluorescent materials including quantum dots. These systems were tested in mice for both *in vivo* and *ex vivo* imaging. The tuneable photophysical properties, the remarkable molar absorption coefficient (up to 3 x $10^6$ $M^{-1}$ $cm^{-1}$, in the 750–850 nm excitation window) and fluorescence quantum yield comparable to that of QDs, constitute important added values for their use in the field of medical diagnostics. These nanoparticles were designed to have two separate emissions (NIR + red), to present suitable characteristics for both *in vivo* imaging and *ex vivo* microscopy in the same NP, a feature unattainable with QDs.

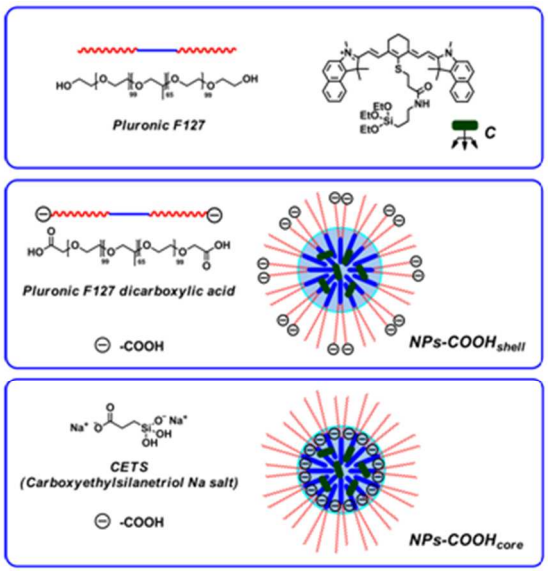


**Fig. 5** Components used during the synthesis, and schematic structure of nanoparticles characterized by different positioning schemes of negative groups ($-COO^-$). NPs-$COOH_{shell}$: -COOH groups were introduced using co-aggregates of Pluronic F127 and a Pluronic F127 dicarboxylic acid derivative as a template. NPs-$COOH_{core}$: -COOH groups were introduced after NPs formation, through condensation of CETS into the silica core. In both cases **C** was used as doping dye and TEOS as silica precursor. Reprinted with permission from ref. [42]. Copyright 2013 American Chemical Society.

In addition, thanks to rhodamine B their use was extended to the two photon microscopy technique ($\lambda_{ex}$ = 980 nm, $\lambda_{em}$ = 610 nm) for the visualization of blood vessels and the detection of extravasation processes in tumour tissues.[115] The very

encouraging results obtained also highlighted the need for a much deeper investigation of these materials in terms of cytotoxicity and cell internalization properties. We therefore investigated the effects of surface functional groups (PEG, -COOH, -$NH_2$) on cell endocytosis and cytotoxicity for Plus NPs doped with rhodamine B.[65] These samples were obtained starting from co-aggregates of Pluronic F127 and of the corresponding di-substituted surfactants.

Functionalized samples presenting external amino- or carboxy-groups did not exhibit appreciable cytotoxicity in several normal or cancer cell types ([NPs] = 100 nM), growing either in suspension or in adherence. Flow-cytometry studies, on the other hand, revealed different responses of the tested samples, demonstrating that amino functionalized nanoparticles exhibit the most efficient kinetics of cell adhesion and internalization, with remarkable levels of nanoparticle cell associated fluorescence persisting for more than 48 hours. With Plus NPs presenting external amino groups we were also able to demonstrate cell endocytosis by a caveolate-mediated pathway. Cell internalization allowed in this case the traceability *in vivo* of leukemic cells.[65]

All these features indicated that these structures could be implemented for NIR imaging and we have recently shown how they are suitable for sentinel lymph node mapping for cancer diagnosis.[42] We carried out a rigorous characterization of two families of NIR emitting covalently Cy7 doped nanoparticles to demonstrate how the surface chemistry of core-shell silica-PEG systems could determine the efficiency of *in vivo* lymph node mapping. We succeeded in synthesizing nanoparticles characterized by different positioning schemes of negative groups (-$COO^-$, Fig. 5): a first system presented quite mobile carboxylate groups at the periphery of the PEG shell, while, in a second system, they were tightly bound onto the silica core and shielded from the external environment by the PEG shell. These samples presented quite constant silica core diameters (10-12 nm), but hydrodynamic diameters spanning the 30-70 nm range and different ζ-Potential values (from -5.0 to -14.0 mV). These different hydrodynamic behaviours, together with the tuning of the position and number of charges in the core-shell nanostructure, proved to influence nanoparticle kinetic behaviour and consequently their lymph node mapping capability. We demonstrated that nanoparticles bearing negative charges buried by a PEG shell were more efficient in NIR mapping of regional lymph in mice than those having a similar dimension and ζ-Potential but with the charges exposed to the external environment, most likely due to their even lower interactions with proteins. We found also that these systems were non-toxic both *in vitro* and *in vivo* and that they underwent efficient excretion by the hepatobiliary mechanism, thus excluding accumulation in the body and long-term toxicity effects. Other strategies can be designed, however, to "cross-link" a surfactant aggregate or co-aggregate to have a nanoparticle with a core-shell silica-PEG structure. In a recent example, bordering between polymer chemistry and silica nanoparticle development, Müller and co-workers synthetized amphiphilic block copolymers by means of RAFT polymerization (Fig. 6).[177] These polymers consisted of a hydrophilic poly-oligo(ethylene glycol) acrylate segment and a second hydrophobic block containing trimethoxy-functionalized and dye-substituted monomers (1-pyrenebutyl acrylate and (3-acryloxypropyl)-trimethoxysilane). The trimethoxysilane moiety upon cross-linking formed a silsesquioxane network, yielding nanoparticles with a final hydrodynamic diameter spanning from 28 to 50 nm. RAFT polymerization was a very valuable choice in this case, as it allowed to polymerize many kinds of monomers controlling their end group functionality, and was mediated by an alkyne-carrying chain transfer agent followed by copper-catalyzed alkyne-azide click chemistry. Oligo(ethylene glycol) acrylate conferred excellent protein repellence abilities and very good water suspendability. The presence of external alkyne was demonstrated by clicking azido-rhodamine B onto the polymer aggregate ends. These nanoparticles exhibited excellent fluorescent properties typical of pyrene moiety and their use as biomarkers within cells was verified by epifluorescence and confocal microscopy, while nanoparticle toxicity was verified by mitochondria toxicity test (MTT) assays.

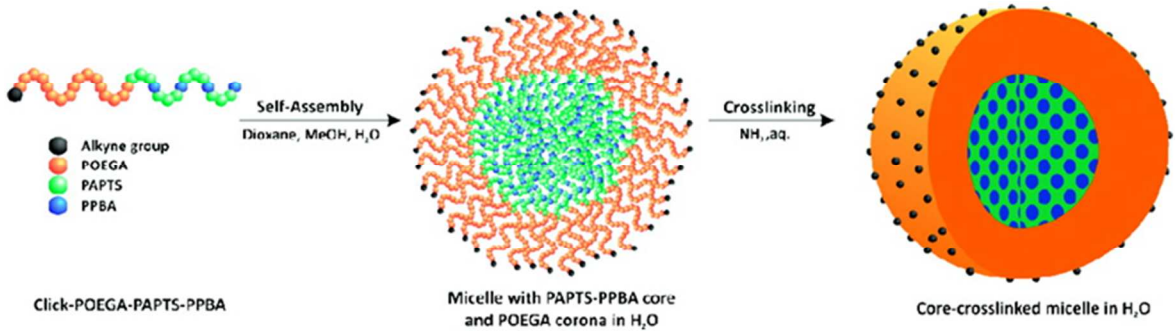


**Fig. 6** Synthetic approach for the fabrication of near monodisperse hybrid nanoparticles via RAFT polymerization and self-assembly in water. Reprinted with permission from ref. [177]. Copyright 2010 American Chemical Society.

A subsequent level of complexity is represented by targeted systems, capable of selectively binding biological molecules or cell sites. Targeting capability can be conferred to fluorescent silica nanoparticles with functionalization with several moieties: the most common ones are probably aptamers, antibodies, peptides and folate.[59] Aptamers are nucleic acids in single-stranded form, selected from a DNA or RNA pool by repetitive binding of target molecules, a process referred to as SELEX (Systematic Evolution of Ligands by EXponential enrichment).[178] They are extremely versatile, thanks to their ability to target certain biological molecules.[179, 180] Their binding capabilities span from protein to small molecules, with a comparable selectivity to antibodies, but with the additional advantage of being smaller and more robust species. For all these reasons they have gained increasing attention as a very effective tool in bioanalysis.

Functionalization of nanoparticles with aptamers generally requires the presence of complementary functional groups on both partners and it can also be a non-innocent process. The group of Tang and co-workers, for example, demonstrated how the efficiency of aptamer functionalized nanoparticles toward human breast carcinoma MCF-7 cell detection can be influenced by the derivatization strategy that is adopted.[181] They synthesized a set of three samples of $Ru(bpy)_3^{2+}$ (Rubpy)-doped silica nanoparticles (d = 60 nm) via a water-in-oil method, adopting different coupling strategies for the aptamer in the three cases. The first sample was functionalized on the surface through covalent conjugation between amine-labelled MUC-1 aptamer and carboxyl-modified nanoparticles, the second using the biotin-labelled aptamer and avidin-conjugated nanoparticles and the third a biotinylated aptamer, a PEG cross-linker bridging avidin and the nanoparticle. It was found that the probes obtained using a PEG cross-linker were characterized by higher coupling efficiency, both in nanoprobe preparation and targeting capability toward human breast carcinoma MCF-7 cells, demonstrating once again the importance of mobility and hindrance in these recognition processes.

Other authors have proposed a similar approach but with increased complexity, using some kind of nanostructurated spacers to cross-link the fluorescent nanoparticles and the aptamer. This strategy was explored by Zhang and co-workers who synthesized "core-satellite" structures, made up of amino functionalized Rubpy-doped silica nanoparticles (d = 60 nm) decorated with several 5 nm citrate stabilized gold nanoparticles.[182] The nanoparticle assembly (Fig. 9) was mediated by amine-citrate exchange on the surfaces, bearing a final structure with a hydrodynamic diameter of 70 nm. Aptamer functionalization was achieved by ligand exchange on the gold surface using thiol-functionalized aptamers. Interestingly, gold nanoparticle decoration caused only very limited effects on luminescence.

Cell fluorescence imaging demonstrates the efficacy of the aptamer modified nanoparticles in labelling MCF-7 cancer cells and low levels of cytotoxicity (cell viability > 97 %) were measured through MTT assay performed on MCF-7 and HEK293T cells over a period of 24 to 48 h.

To find sensitive and rapid methods to implement the current diagnostic protocols, detecting multiple cells for example, is a stringent need in relation to achieving fast and economical strategies. To reach this goal, the group of Tan and co-workers developed aptamer-conjugated nanoparticles to perform the extraction of different cancer cells in a single analysis, using high-affinity DNA aptamers for recognition.[183]

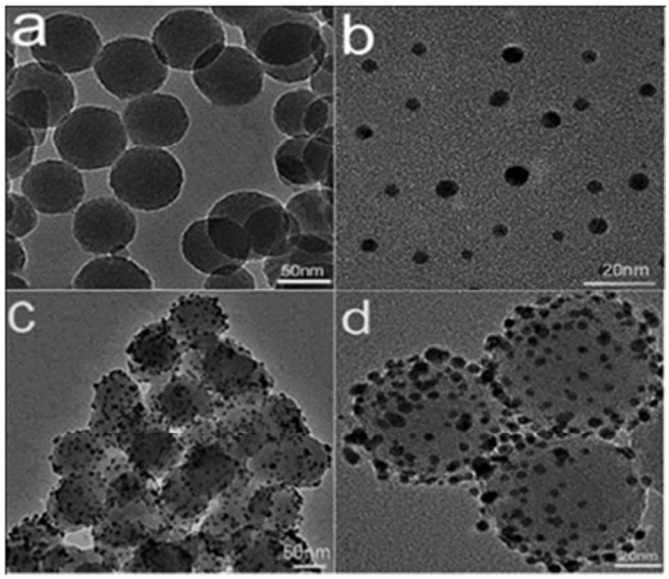


**Fig. 9** TEM images of (a) Rubpy-dye-doped silica (DySiO2) nanoparticles, (b) citrate-stabilized Au NPs, (c) Low- and (d) High-magnification TEM images of DySiO2–(Au)*n* core-satellite nanospheres. Reprinted from ref. [182] with permission from The Royal Society of Chemistry.

They used the 88-base oligonucleotide sequence for CCRF-CEM acute leukaemia cells together with two other different oligonucleotide sequences with specific binding properties for cell lines of Burkitt's lymphoma (Ramos) and non-Hodgkin's B cell lymphoma (Toledo). These sequences were conjugated to magnetic nanoparticles and fluorescent silica nanoparticles to allow collection and imaging of the intact cancer cells. Aptamer-conjugated magnetic nanoparticles (d = 65 nm) were used to achieve cell sorting and three fluorescent silica nanoparticles (d = 50 ± 5 nm), doped with Rubpy, tetramethylrhodamine and Cy5 respectively, were synthesized to identify the three different cell lines within the sample (Fig. 10). The limit of detection of this technique resulted in 250 cells using CEM target cells, with a dynamic range of about two orders of magnitude. In the case of mixed cell samples, selective isolation was demonstrated using fluorescence microscopy imaging. The same group extended this approach to the recognition of the same cancer cells in complex samples, introducing aptamer-conjugated fluorescent silica nanoparticles with FRET-dependent emission signatures.[184] The nanoparticles (d = 60 nm) were synthesized with a Stöber procedure, using as doping dyes the APTES derivative of 5-carboxyfluorescein, 5-

 

carboxyrhodamine 6G and 6-carboxy-X-rhodamine. Single-, dual- and triple-dye doped silica nanoparticles with different doping ratios were prepared, allowing the tuning of the emission properties of these materials, which consequently presented different colours under the same excitation ($\lambda_{ex}$ = 488 nm), as the efficiency of the energy transfer was not complete.

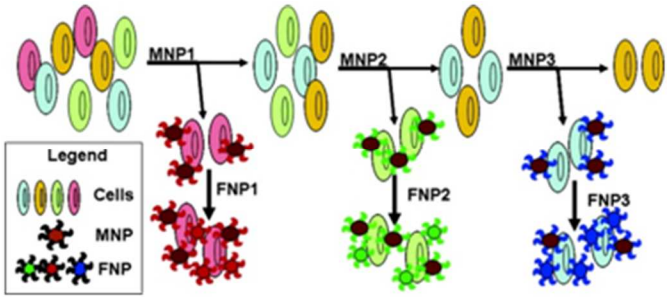


**Fig. 10** Schematic representation of the extraction of cell samples using aptamer functionalized magnetic nanoparticles and DDSNs. Reprinted with permission from ref. [183]. Copyright 2007 American Chemical Society.

The fluorescent nanoprobes were detected by fluorescence imaging and flow cytometry, and the advantage in using FRET-based nanoparticles was to simplify the experimental setup needed for their detection, as a single laser source was needed for their excitation. This system showed high specificity, provided by the aptamers, and signal amplification thanks to the FRET processes occurring in the fluorescent silica nanoparticles.

The examples presented show how DDSNs can be valuable alternatives also to targeted molecular dyes, primarily for the signal gain they can supply, but aptamers are not the only receptors investigated and promising. Another extensively studied general strategy to develop effective probes is to endow nanoparticles with avidin to have the possibility to exploit the versatility of biotin-avidin technology for the bioconjugation of suitable targeting moieties (e.g. antibodies) to the NPs. Tang and co-workers, for example, synthesized 60 nm diameter Rubpy-doped silica nanoparticles using a water-in-oil method, having long-chain carboxyl-terminated functionality on their surface, that were used to conjugate avidin.[185] This system, together with biotinylated rabbit anti-Carcinoembryonic Antigen (anti-CEA) antibody, was used for the recognition of CEA (carcinoembryonic antigen) in human lung carcinoma A549 cells. Anti-CEA antibody funtionalization via covalent binding of Stöber synthesized nanoparticles was exploited also by Song and co-workers, who synthesized FITC and TRITC-doped nanoparticles (d = 80 nm) for the detection of SPCA-1 cells.[185, 186] The *in vitro* cytotoxicity of this system was measured with MTT assay on SPCA-1 cells, showing a cell viability higher than 85%, for NPs concentration up to 80 μg/mL after 24h of incubation.

A conceptually similar approach following a cross-linking strategy comprising BSA, glutaraldehyde and amino functionalized TRITC-doped silica nanoparticles was used to obtain nanoparticles conjugated with the anti-HER2 antibody, to recognize human ovarian tumour (HOT) cells.[187]

In another example, Nooney and co-workers carried out a thorough investigation of the optimization of synthetic conditions for the preparation of FITC-doped nanoparticles with size ranging from 16 to 80 nm, using both ternary and quaternary microemulsion methods.[51] These systems were tested as labels in a fluorescence-based immunoassay for the detection of human IgG and human chorionic gonadotropin after conjugation of anti-hIgG and anti-αhCG to the NP surface using PAMAM dendrimer linkers. They showed lower limits of detection and better coefficients of variance than the free dye.

Another strategy to target nanoparticles, also *in vivo*, is surface functionalization with the folate-folate receptor pair. Belfield and co-workers, for example, developed a two-photon absorbing and aggregation-enhanced near-infrared emitting pyran derivative embedded in silica nanoparticles. This strategy by-passed the frequent quenching problems that reduce the bioimaging capabilities of nanoprobes with high chromophore loading. The surface of these nanoparticles was functionalized with folic acid and *in vitro* studies confirmed their uptake by HeLa human cervical cancer cells. Following intravenous injection, they specifically homed to HeLa tumour xenografts in mice, which were internalized by the tumour cells. Two-photon fluorescence microscopy bioimaging provided 3D tumour imaging up to a depth of 350 μm.[188]

### 3.2 Multimodal NPs

The versatility of silica nanostructures allows an easy integration of different functions in a single nano-object, as already anticipated in the introduction. This approach has been exploited by many research groups to prepare materials suitable for multi modal imaging by combining different signals, e.g. fluorescence, MRI, PET and Raman spectroscopy. As far as dual mode nanoprobes are concerned, the *in vitro* delivery of a system suitable for fluorescence and MRI detection exploiting the luminescence and paramagnetic properties of Tb(III) and Gd(III) ions, respectively, was demonstrated for different cancer cell lines, e.g. SGC7901 gastric cancer cells and NCI-H460 lung cancer cells. These NPs were obtained by doping a 16 nm silica carbonate core with the emissive metal ion and they showed no toxicity, at least at the experimental doses used.[189]

Tan *et al.* achieved the same dual modality preparing a uniform and stable nanosystem by integrating a set of fluorescent conjugated polymers and super-paramagnetic iron oxide nanocrystals into silica (Fig. 7). They tested its imaging abilities in labelling cultured human liver cancer cells and the magnetic properties of the resulting nanocapsules were further exploited to magnetically guide them into the cells.[190]

Besides the study of the efficacy of these kinds of materials, it is extremely important to investigate their mechanisms of endocytosis and toxicity. Corsi *et al.* explored, in this sense, three kinds of model magneto-fluorescent NPs in MCF-7adenocarcinoma cells.[191]

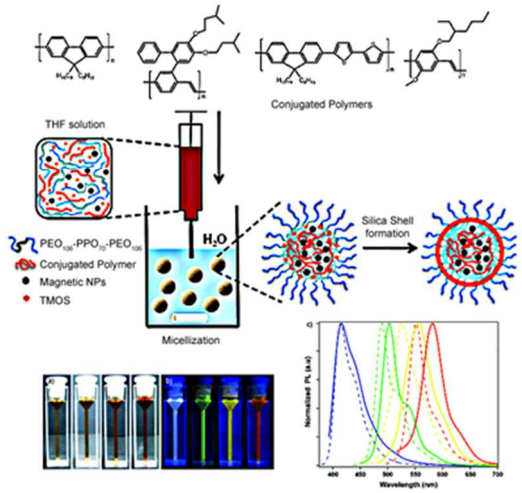


**Fig. 7** Synthetic scheme for the formation of bifunctional magnetic fluorescent silica nanocapsule (BMFSNs). Chemical structures of the doping conjugated polymers. Photoluminescence spectra of the aqueous dispersions of loaded BMFSNs (solid lines) and of conjugated polymer solutions in THF (dashed lines). Reprinted with permission from ref. [190]. Copyright 2011 Wiley Publishers Ltd.: *Chemistry A European Journal*.

These NPs were first assessed in terms of size, morphology, ζ-potential, fluorescence efficiency, capability of enhancing T2 relaxivity of water protons and stability. The authors reported that, besides the well-documented size effect, the ionic charge seemed to be a crucial factor for particle internalization, as penetration through the cell membrane could be modulated by the surface charge. TEM and confocal microscopy reveal that NPs are internalized by clathrin-mediated endocytosis and macropinocytosis. Hence the NPs follow a physiological pathway of internalization once incorporated by the cell. Moreover they display no relevant cytotoxicity in vitro.

Also Niu *et al.* investigated the cytotoxicity of novel, thiol-functionalized, fluorescent in the visible range, and super-paramagnetic silica composite NPs on three other typical cell lines (HUVEC, RAW264.7, and A549).[192] These NPs have monodisperse sub-100-nm size in aqueous solution and they showed complete lack of toxicity in *in vitro* experiments. Moreover, the authors demonstrated that these NPs can be used as a new class of magnetic resonance imaging (MRI) probes, having a remarkably high spin–spin (T2) relaxivity (Fig. 8).

The dual-modality nano-probe prepared by Bumb and co-workers coupled the magnetic properties of ultra-small super-paramagnetic iron oxide nanoparticles (USPIOs) again but with a near infrared flurophore (Cy5.5) better suited to imaging applications.[193] The probe, having a final diameter of ~17 nm, was prepared by surrounding the iron oxide core with a dye-doped silica shell. These final silica-coated iron oxide nanoparticles (SCION) were characterized by TEM, DLS and a superconducting quantum interference device (SQUID). They then investigated the leakage into subcutaneous A431 tumours in mice of these NPs, which have a strong negative surface charge and are stable in the physiological pH range. The authors showed that these NPs accumulated in leaky tumours by the Enhanced Permeability and Retention effect (EPR) and then cleared from the tumours within 24 hours post-injection, demonstrating good potential for *in vivo* diagnostic applications. Conjugation to targeting ligands is expected to lead to accumulation in leaky tumours, clearance of non-specific uptake and imaging with minimal background within times such as 24h post-injection.

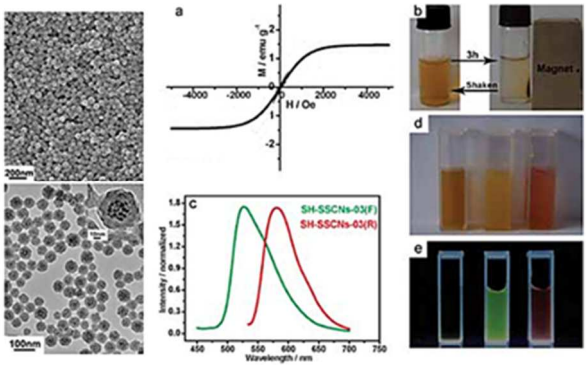


**Fig. 8** FE-SEM and TEM images of thiol-functionalized, fluorescent and super-paramagnetic silica composite NPs (left), and (a) their representative field-dependent magnetization at 300 K. b) Magnetic NPs driven by an external magnet in water. c) Photoluminescence spectra of FITC ($\lambda_{ex}$ = 430 nm) and RITC ($\lambda_{ex}$ = 520 nm) doped nanoparticles. d) From left to right: undoped NPs, FITC and RITC doped nanoparticles. e) Same dispersions in water under UV light. Reprinted with permission from ref. [192]. Copyright 2010 Wiley Publishers Ltd.: *Adv. Funct. Mater.*

There are other examples of *in vivo* studies of NIR emitting nanoparticles and in particular Kim *et. al.* obtained the enhancement of the fluorescence of a near infrared dye (NIR797) encapsulated into magnetic silica nanoparticles labelled with Gallium 68 as a radiotracer. The resulting PET/MRI silica nanoprobe was injected into the forepaw of mice providing multimodal *in vivo* imaging of sentinel lymph nodes and demonstrating high fluorescent intensity and stability.[194]

We would also like to present an example of an untargeted probe that combines the dual capability of X-ray computed tomography (CT) and fluorescence imaging.[195] The fluorescence of the nanostructures arises from the loading with Indocyanine green of mesoporous silica-coated gold nanorods that are suitable contrast agents for X-ray computed tomography (CT). The NIR fluorescence of these NPs can be detected up to 12 h post intratumoral injection and, according to the authors, offers a versatility that can be exploited to obtain multiplexed images in an easier way in comparison to traditional contrast agents.

Targeted fluorescent and MRI contrast agents were obtained surrounding $Fe_3O_4$ cores with a fluorescein-doped $SiO_2$ shell functionalized with hyperbranched polyglycerol ending with folic acid moieties, and the final NPs resulted with a diameter of circa 50 nm (Fig. 11). These targeted NPs can find a potential use for real-time imaging in ovarian cancer resection, as they can be simultaneously detected by MRI and

 

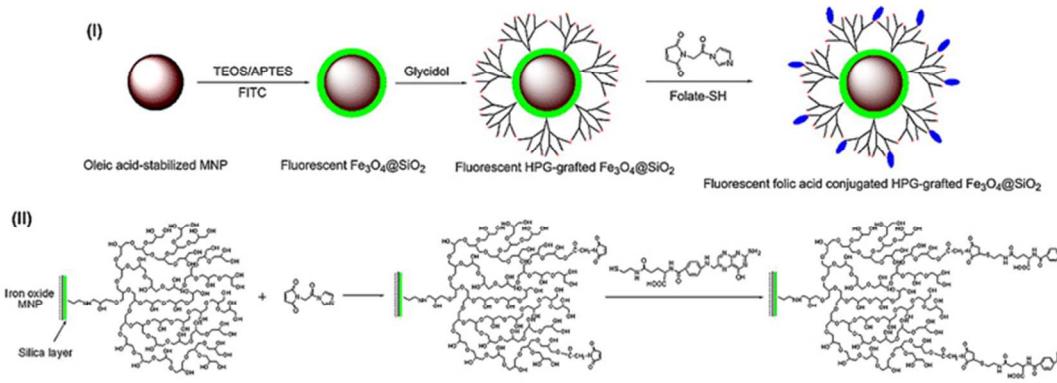


**Fig. 11** Synthetic scheme of folic acid-conjugated hyperbranched glicidol $Fe_3O_4$@$SiO_2$ fluorescent nanoparticles. Reprinted with permission from ref. [196]. Copyright 2011 Elsevier: *Biomaterials*.

fluorescence microscopy and the authors have shown that they are preferentially uptaken by human ovarian carcinoma cells (SKOV-3), in comparison with macrophages and fibroblasts.[196] The same target moiety was used by H. Yang *et al.*[197] to conjugate amino functionalized silica-coated manganese oxide NPs (d = 35 nm) together with the rhodamine B isothiocyanate dye. The use of these nanocomposites was tested with several techniques (flow cytometry, confocal microscopy, and MRI) demonstrating that they can specifically target cancer cells over expressing folate receptors.

Among the targeted multimoldal NPs exploiting antibodies (ABs) against trans-membrane receptors overexpressed in cancer cells, the clinical antibody cetuximab, for example, was conjugated with magneto-fluorescent silica NPs. The ferrite core was surrounded by a silica-PEG/rhodamine B layer to allow the targeting and imaging of colon cancers that overexpress the epidermal growth factor receptor. In particular, specific fluorescence due to cetuximab-conjugated magneto-fluorescent NPs was detected *in vivo*, in parallel to significant MRI signal changes in the case of targeted HCT-116 human colon carcinoma cell subcutaneous xenografts.[198] It is however important to highlight the fact that, even when the nano-probe is functionalized with targeting moieties, the presence of background signals arising from non-specific interactions cannot be completely eliminated.

An elegant and efficient way to overcome this problem and to obtain a potential improvement of the signal-to-noise ratio, can be to design NPs with fluorescence activated only by the target binding through an enzymatic process. This kind of smart targeting of the tumour microenvironment was demonstrated by Cha and co-workers exploiting tumour metallopeptidase 2 and a specific enzyme substrate bioconjugated with cyanine 5.5 (Fig. 12).[199] The dye molecules were bound to a thin silica-PEG shell on the surface of iron oxide NPs that caused an almost complete quenching (97.2 % efficiency) of their fluorescence. A protease specific fluorescence recovery was observed *in vitro* due to the specific peptide cleavage by MMP-2, with a sensitivity of 0.5 nM. The modification of commercial NPs (d = 50 nm) was the approach chosen by D. W. Hwang *et al.*[200] to design a tri-modal cancer-targeted imaging system for *in vivo* fluorescence, radionuclide and MR imaging.

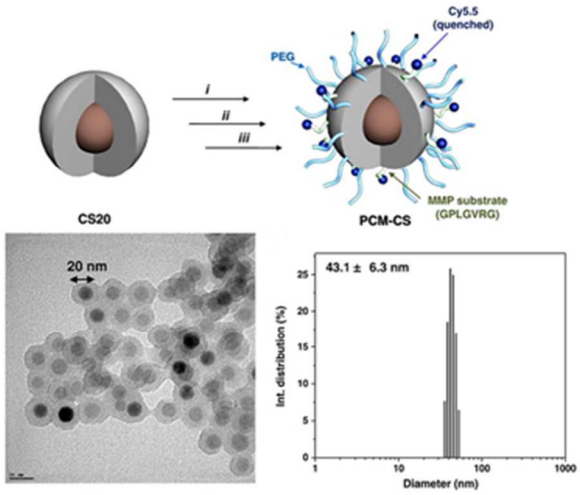


**Fig. 12** Structural scheme of the multimodal core-shell nanoparticles PCM-CS, TEM images and size distribution by dynamic light scattering. Reprinted with permission from ref. [199] Copyright 2011 Elsevier: *J. Controlled Release*.

Such NPs, that have a core-shell structure with a cobalt–ferrite nucleus and a rhodamine-doped carboxy-functionalized silica external layer, were conjugated with AS1411 aptamer (MF-AS1411), a moiety which targets nucleolin, a cellular membrane protein highly expressed in cancer. To allow a third detection method, the surface of the NPs was further modified with a specific ligand capable of chelating $^{67}$Ga-citrate. The ability of the resulting NPs to label nucleolin-expressing C6 cells in a specific way was confirmed *in vitro* by confocal microscopy analysis. Systemic injection in mice was followed by radionuclide imaging and confocal fluorescence microscopy

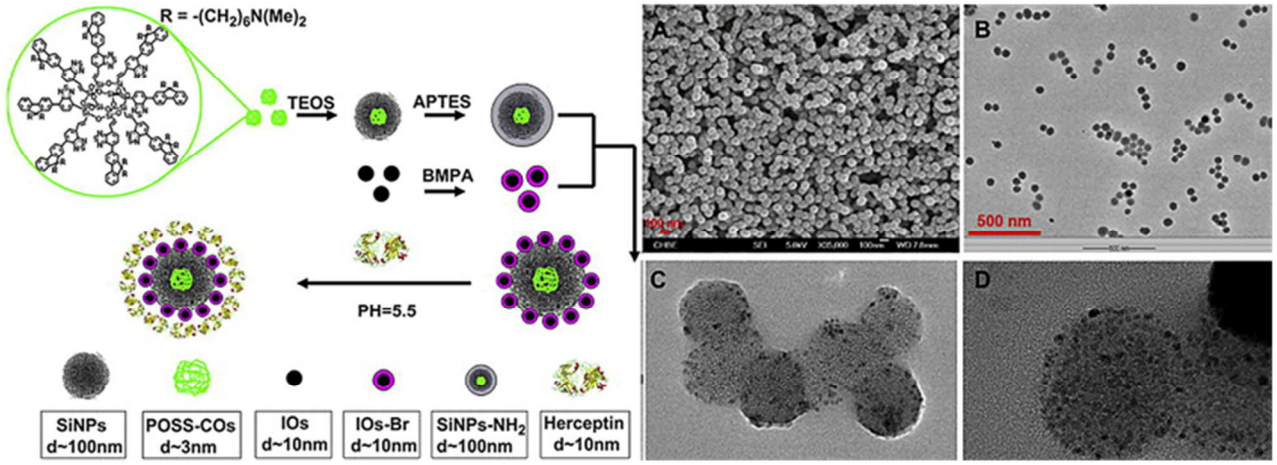


**Fig. 13** Scheme of polyhedral oligomeric silsesquioxanes (POSS) scaffold of hydrophobic conjugated oligomers loaded into the silica nanoparticles; Iron oxides (IOs) nanoparticles conjugation to the silica surface and adsorption of herceptin. (A) FESEM image and (B) TEM image of the POSS-COs loaded silica NPs with no IO layered on the nanoparticle surface. (C) and (D) are the TEM images of the POSS-COs loaded silica NPs of the Fe3O4 IO surface layer. Reprinted with permission from ref [201] Copyright 2011 Elsevier: *Biomaterials*.

to test their performances *in vivo*. Unfortunately these experiments highlighted severe non-specific liver accumulation of these NPs by the mononuclear phagocytic system, an unexpected behaviour for NPs covered with the stealth PEG moieties that usually increase circulation time. Circulation time is, in fact, a very important factor connected both with the time of measurement and the possibility to follow circulating cells. Y. Mi *et al.*[201], for example, proposed the use of a dual mode nano-hybrid with an overall diameter of 100 nm and a ζ-Potential value of 12 mV to sort and detect circulating tumour cells using immunomagnetic methods or microfluidic devices (Fig. 13). The final NPs showed quite low cytotoxicity towards SK-BR-3 cancer cells and NIH/3T3 fibroblast cells, with an essential contribution of herceptin to cellular uptake and selective detection. In the design of the nanostructure, iron oxide NPs were grafted onto the surface of mesoporous silica nanospheres loaded with a polyhedral oligomeric silsesquioxanes scaffold of hydrophobic conjugated fluorescent oligomers. Further functionalization with the targeting ligand herceptin (Trastuzumab) was achieved via simple adsorption. This ligand is able to recognize the receptor HER2, which is over expressed in 25-30% of invasive breast cancer cells.

A different strategy was applied by Lee *et al.* for the development of a new generation of nanoprobes that merge multiple fluorescent dyes and multiple magnetic nanoparticles into a single structure.[202] According to the authors, this approach provides superior fluorescence and MR imaging capabilities through the synergistic enhancement of their respective components. The resulting dual functional NPs have a "core–satellite" structure comprising a dye-doped silica "core" and multiple "satellites" of magnetic nanoparticles. Optical and MR imaging of neuroblastoma cells expressing polysialic acids (PSAs) was achieved after functionalization of the NPs with HmenB1 antibodies as targeting agents. PSA is a marker not only of neuroblastoma but also of lung carcinoma and Wilms' tumours; this carbohydrate is also associated with neural pathways, such as synaptic plasticity, learning and memory, and cell-to-cell interaction.

### 3.3 NPs for PDT and PTT

Fluorescent silica nanoparticles, are frequently provided with additional components to confer therapy capabilities. These are mainly drug release, Photo Dynamic Therapy (PDT) and Photo Thermal Therapy (PTT). It is worth noting here that the design of PDT[203] and PTT[203, 204] systems is very close to that of fluorescent silica nanoparticles, as no release of the photothermal or photosensitizer agent is needed (or desired) to perform the required function.

Fluorescent silica nanoparticle designed for PDT applications usually contain a photosensitizer, i.e.: a molecule that, upon irradiation with light, is able to generate reactive oxygen species such as cytotoxic singlet oxygen. The incorporation of a PDT agent in a colloidal carrier is advantageous for several reasons; for example, they are usually dyes, such as porphyrins, with limited solubility in biological environment, and inclusion in a nanoparticle is an elegant way to take them in water.[98, 205]

It has to be underlined, however, that a crucial aspect in PDT is the possibility to have an efficient energy transfer from the excited state (typically, a triplet state) of the photosensitizer to molecular oxygen, whose fast diffusion into the silica matrix represents a fundamental parameter in these NPs. This process, as already mentioned, depends on the synthetic procedures, since in many silica NPs the quenching by oxygen is strongly prevented.[77, 86]

 

Besides this, even non-targeted nanoparticles undergo passive accumulation in tumour tissues due to the EPR effect,[206] and since several photosensitizer molecules can be contained in a single nanoparticle, a therapeutic gain is possible. However, the need to prevent the sensitizer leaching from nanoprobes has been evidenced by the group of Prasad[105] and later by Mancin and co-workers.[207] Despite poor solubility, in fact, photosensitizer release from the particle can be promoted by the interaction with proteins and lipophilic districts within the body. For this reasons, after pristine examples of PDT agents embedded within ORMOSIL nanoparticles,[98] Prasad and co-workers prepared a similar structure (d = 20 nm) for PDT treatment of cancer, with the 3-Iodobenzylpyro-silane photosensitizer covalently linked.[101] This dye retained its spectroscopic properties and generated cytotoxic singlet oxygen upon photo-irradiation. The covalent binding prevented the release during *in vitro* testing, over Colon-26 and RIF-1 cells, with an amount of nanoparticles corresponding to a sensitizer concentration of 2 and 0.5 μM respectively. Cell viability was measured with a MTT assay immediately after the light treatment and a cell survival of less than 20% was highlighted.

Another way of hampering photosensitizer release from ORMOSIL nanoparticles was described by Mancin and co-workers, who showed how a PEG passivating layer can be an alternative strategy for limiting interactions with serum protein and, consequently, photosensitizer release.[100] They synthesized two different samples of 33 nm diameter ORMOSIL nanoparticles doped with meta-tetra(hydroxyphenyl) chlorine (mTHPC), with and without external PEG functionalization. The comparison between the cellular uptake and phototoxic activity *in vitro* of mTHPC toward the cell line KYSE 510 (human oesophageal squamous carcinoma) showed that nanoparticle surface coating with PEG largely prevented the transfer to proteins and then the release of the photosensitizer from the system. Nanoparticle localization through fluorescence measurement was made possible by the covalent doping of the organosilica matrix with an alkoxysilane eptamethine dye.

Other groups, such as Wang and co-workers, have exploited other kinds of nanoparticle surface modification and composition to prevent PDT agents from leaching. They synthesized PDT active nanoparticles (d = 100 nm) doped with methylene blue, a water soluble NIR emitting sensitizer[208] via a water-in-oil microemulsion, using TEOS and trihydroxyl silyl propyl methyl phosphonate as silica precursors. Phosphonate groups conferred a very negative ζ-Potential (-44.0 mV) to these nanoparticles and, probably due to strong electrostatic interactions between them and the dye molecules, methylene blue leaching was reduced in serum within eight hours to less than 1% of the pristine doping regime. Another important consequence of encapsulation was to prevent its enzymatic degradation to leukomethilene blue, a PDT inactive molecule. The PDT activity was measured *in vitro* on Hela cells at several nanoparticle concentrations, showing a cell survival of less than 20% after irradiation and a relatively low dark citotoxicity. The authors also performed *in vivo* PDT experiments on mice presenting implanted tumours, treating the mice with intratumoral injections of a nanoparticle suspension. Light irradiation of tumours bearing nanoparticles led to gradual tissue necrosis, suggesting the efficacy of this theranostic system.

It is however expected that, in systems that contain luminophores to allow fluorescence imaging, a straightforward strategy could be to take advantage of the same or similar species to also perform light-based therapies such as PDT and PTT. Qiao and co-workers reported an example of triple-functional NPs for theranostics based on PDT. They prepared core-shell structured silica-based nanomaterials that coupled MRI and luminescence imaging. The NP core had a diameter of 10 nm and was made of rare-earth oxide (Ytterium, Gadolinium, Erbium) which behaved like an up-conversion nanophosphor surrounded by a silica shell covalently functionalized with a photosensitizer (hematoporphyrin or silicon phthalocyanine dihydroxide). Thanks to the up-conversion phenomenon, these NPs showed, upon excitation at 980 nm, high energy emissions centred at 550 nm and 660 nm. The former peak was used by the authors as a fluorescence signal for imaging while the latter was used to excite the photosensitizer, leading to singlet oxygen generation that killed HeLa cancer cells *in vitro*. As far as the signal for MRI is concerned, the Gadolinium(III) present in the inner core allowed a good contrast, showing performances comparable to commercial clinical agents.[209]

Other authors used the already mentioned methylene blue as photosensitizing drug for singlet-oxygen generation, including it in a silica shell surrounding label-tagged gold nanostars suitable for surface-enhanced Raman scattering (SERS) detection.[210] The gold nanostars were tuned for maximal absorption in the NIR spectral region and functionalized with an NIR dye for surface-enhanced resonance Raman scattering (SERRS). The final NPs gave a dual signal: SERS from the Raman dye was observed upon excitation at 785 nm, while fluorescence from methylene blue itself was detected upon excitation at 633 nm. Methylene-blue-encapsulated NPs showed significant singlet-oxygen generation and had a cytotoxic effect on BT549 breast cancer cells upon laser irradiation.

F. Wang *et al.*[211] followed a reverse microemulsion strategy to prepare another multimodal system with multiple core-shell architecture for PDT, by coating a 6 nm diameter $Fe_3O_4$ core with an FITC-APTES-doped silica shell of ~ 17 nm of thickness. In a second step, a mesoporous silica external layer was added and covalently doped with aluminium phthalocyanine ($AlC_4Pc$) as the PDT agent and conjugated with folic acid as the targeting ligand. Human hepatoma cells (QGY-7703) were then used as a model to demonstrate the cellular uptake of these NPs and their good performance as imaging agents, while human hepatocyte cells (QSG-7701) were used for relative cell viability measurements. By comparing different systems the authors showed that the presence of folate leads to a preferential uptake of the NPs in HeLa cells and, as a

consequence, to more efficient promotion of Hela cell death by PDT.

In the field of PDT, metallo-porphyrins are one of the most frequently studied active species and they have been used also in these kinds of nanoprobes. For example, Lo and co-workers reported the synthesis and application of multifunctional NPs based on Pd-porphyrin as photosensitizer.[212] The first step of the NPs design was the preparation of the fluorescent component: a mesoporous silica core doped with an NIR emitting dye, ATTO647N. The photosensitizer was then included by simple adsorption into the nanochannels of the mesoporous nanostructure and, in the last step, the peptides cRGDyK were added as targeting units for αvβ3 integrins, typically overexpressed in cancer cells. The efficiency of these NPs as PDT agents was demonstrated in the case of MCF-7 human breast cancer cells and U87-MG human glioblastoma cells.

Although less common, another light driven therapy exploited in theranostic colloidal nanosystems is PTT. It is based on photoablation processes obtained by strong light absorption with concomitant release of heat at microscopic level. In most cases, PTT agents are low emitting molecular dyes[213] or metallic nanostructures, as they must present efficient non-radiative deactivation leading to heat dissipation.[72] In the latter case, gold is usually the metal of choice due to its stability, synthetic accessibility and low toxicity,[214, 215] but it is also a well-known quencher thanks to gold plasmon interactions with neighbouring luminophores.[216] For this reason, luminescent gold-based systems are not frequent. In a quite recent example however, Moudgil, Grobmyer and co-workers succeeded in preparing 50 nm luminescent silica nanoparticles covalently doped with FITC or rhodamine B derivatives and speckled with 1-5 nm, NIR absorbing, irregularly shaped gold deposits on their surface.[217] These nanoparticle were prepared following a reverse microemulsion strategy, using, together with TEOS, aminopropyltriethoxy silane to stabilize gold nanoparticle growth on the silica surface. This system presented retention of the luminescence of the dyes, also visible to NIR absorbance. Their fluorescence and photothermal ability were demonstrated *in vitro* on lung A549 cancer cell line, upon laser irradiation at 785 nm, and also *in vivo* with intratumoral injection of nanoparticles in nu/nu tumour bearing mice. These experiments showed a doubling of the necrosis percentage on the nanoparticle-treated tumours, a result that is favourable to future clinical and theranostic applications of these systems.

Another possible way to develop theranostic nanomaterials with fluorescent and nonplasmonic photothermal structures is to use a multi-dye-doped silica nanoparticle presenting efficient compartmentalization of the different kinds of dye. Mesoporous nanomaterials properly fit this purpose as the fluorescent dye can be embedded in the silica matrix while the PTT agent can be loaded into the nanochannels. Following this strategy, Grobmyer and co-workers developed a mesoporous system (average size of 105 ± 16 nm, average pore centre-to-centre distance of 3.6 nm) doped with near infrared fluorescent heptamethine cyanine dye IR780-APTES and containing metallo-naphthalocyanine loaded into the pores.

These nanoparticles were studied *in vivo* using a direct tumour injection model. Remarkable brightness was measured with a 300-fold enhancement in quantum yield versus free dye, and laser excitation of the naphthalocyanine promoted photothermal activity. As a result, tumours co-injected with the nanoparticles were easily visualized, and significant tumour necrosis (95 %) was induced upon photothermal ablation.[218]

### 3.4 NPs for drug delivery

Many different molecules have been proposed as anti-cancer loading materials for theranostic NPs, but doxorubicin is most often used for a number of *in vivo* applications. This is due partly to the fact that this drug, thanks to its hydrophilicity, can be easily embedded in silica-based materials, as reported by Chen *et al.* in the case of hollow mesoporous silica NPs functionalized with fluorescein and manganese oxide, an MRI contrast agent with pH-dependent resonance. Due to the acidity of the environment of cancer tissues, the relaxation rate of manganese oxide, which is already higher than that of commercial gadolinium derivatives, undergoes an 11-fold increment. Moreover, hollow NPs behave like ultrasonographic contrast agents and release the doxorubicin cargo intracellularly, showing a strong *in vitro* anti-proliferative effect.[219]

The ability of multifunctional biocompatible and water-soluble magnetic NPs to deliver doxorubicin into the cytoplasm was also investigated by Lu and co-workers.[220] These NPs, used to target Human hepatoma 7402 and H446 lung cancer cell lines, consist of a mesoporous scaffold with a core-shell structure functionalized both with a polymeric derivative of a fluorescent moiety and with folic acid as the cancer targeting part. The author concluded that their mesoporous NPs coated with the fluorescent polymer had excellent drug-loading efficiency, favourable biocompatibility (cell viability above 85% at high concentration) and dispersibility under physiological conditions. Moreover, thanks to the folate moiety on the surface, these NPs target the tumour cells and are efficiently internalized, a process that can be tracked by exploiting either the superparamagnetic iron oxide core or the fluorescent polymeric shell. Sustained release of the loaded drug was observed over 100 hours under *in vitro* conditions.

## 4. Silica nanoparticles in non-cancer research

Cancer diagnosis and treatment has been the area that has attracted the largest research effort in the application of SiNPs. Their use, however, is not at all limited to this field but spans the diagnosis and imaging of many other diseases, and particularly those that have bacteria and viruses as etiologic agents. It has been estimated that, every year, in the United States, 76 million illnesses, with circa 300000 hospitalizations, and over 5000 deaths can be attributable to foodborne illness.

Many of these pathogenic situations are likely originated by bacterial infection.[95]

The situation is even more severe in developing countries. Their correct and timely identification is of crucial importance, as it can guide treatment options and help to determine appropriate and successful therapies.[221] In addition, the possibility to detect the presence of pathogenic agents is also essential for fighting bioterrorism.[222] Conventional methods are usually labour intensive and time consuming, involving culture enrichment followed by serological, biochemical tests or DNA/RNA characterization. Therefore, the development of new rapid and sensitive methods is of great importance.

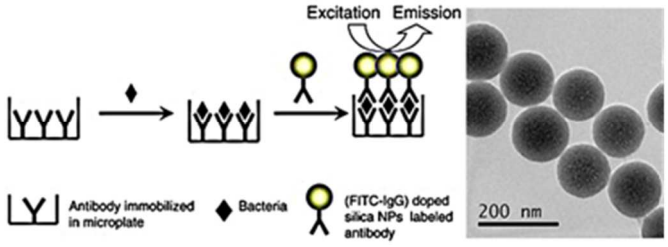


**Fig. 14** Schematic illustration of sandwich-type immunoassay of *Listeria monocytogenes* with bioconjugated fluorescent silica nanoparticles (left) and TEM image of (FITC-IgG)-doped silica nanoparticles. Adapted from ref. [223]. Copyright 2011 Elsevier: *Journal of Microbiological Methods*.

In this context, Wang *et al.* have developed a sandwich-type immunoassay to detect Listeria monocytogenes, a ubiquitous food-borne pathogen (Fig. 14).[223] This method is based upon SiNPs doped with fluorescein and bioconjugated with IgC, obtaining a rather high sensitivity with a detection limit of 50 CFU/mL. Another sandwich assay was also developed by Li and Xu,[221] to monitor the presence of Shigella flexneri, known as the causative agent of bacillary dysentery, which is an endemic disease in developing countries such as Bangladesh, China, Pakistan and Indonesia. Their method starts from the immobilization on a slide of Concavalin A, which interacts specifically with bacterial cell walls containing glycosidic residues associated with tecichoic acid. The FICT-doped and antibody-coated nanoparticles (diameter of circa 50 nm) can then react with the specific bacteria and signal the presence of the target. The methodology was also tested successfully on human faecal samples.

Ekrami *et al.*, on the other hand, directed their attention to Mycobacterium tuberculosis (M. tuberculosis), which is the main etiology of tuberculosis, a public health problem of global importance. According to the World Health Organization, in 2009 there were an estimated 9.4 million incident cases of tuberculosis worldwide and approximately 1.7 million people died of tuberculosis in that year.[224] The gold standard for the diagnosis of tuberculosis is, also in this case, the cultivation of the bacterium, a method that can allow the detection of 100 bacilli/mL in sputum specimens. Different molecular methods have been developed, offering several advantages in terms of rapidity and sensitivity. However, they are usually expensive and require trained personnel so their implementation is difficult, especially in regions where M. tuberculosis infection is more common. To circumvent these problems, the authors exploited the high brightness typical of DDNPs to try to avoid the amplification or enrichment processes. The DDNPs were prepared in accordance with the Stöber methodology and using the metal complex $Ru(bpy)_3^{2+}$ as the doping dye. The resulting circa 60 nm in diameter Nps were then conjugated with protein A extracted from Staphylococcus aureus, which is capable of binding to the Fc portion of immunoglobulins, especially the IgGs of the target bacteria, in a large number of species. The procedure requires the conjugation of mouse monoclonal anti-M. tuberculosis antibody to the pathogens in the sputum specimen, followed by the addition of DDSNs functionalized with the protein A and thorough washing. The authors tested this assay on a large number of clinical samples proving its diagnostic specificity and sensitivity. Moreover, this is a very fast (2–3 hours) procedure compared with the 6–8 weeks needed for the culture, followed by 5 hours for the nested PCR assay. All these advantages allowed the authors to predict potentially wide usage of the assay in the future.

It is worth noting here that the authors highlighted the problem of the auto-fluorescence exhibited by a few samples, despite the use of filters, as a possible addressable point for further improvements. Interestingly, the use of metal complexes and particularly of $Ru(bpy)_3^{2+}$ can offer a way to overcome all problems related to light scattering and auto-fluorescence through time-gated luminescence, so that specific long-life signals can be selectively imaged over short-lived ones with a high signal-to-noise ratio.[225] Thanks also to the ca. three-fold increase of the excited state lifetime (and, consequently, of the luminescence intensity) observed for $Ru(bpy)_3^{2+}$ when covalently attached to the silica matrix in the DDSNs,[225, 226] luminescent Ru(II) complexes are considered very promising in this context because of their visible-light excitation and emission, large Stokes shift and relatively long luminescence lifetime properties. The increase in sensitivity offered by time-gated luminescence using Ru(II)-DDSNs was interestingly demonstrated by the highly specific imaging detection of Giardia lamblia, a water-borne pathogen that is the cause of diarrheal diseases.[225] We think that this approach can have wide use in the future, also considering that $Ru(bpy)_3^{2+}$ is, as described in this review, one of the most frequently used doping dyes for DDSNs.

Another strategy that has been investigated to increase the signal to noise ratio is based on the derivatization of the surface of DDSNs with dendrimeric structures.[227, 228] In these systems NPs with a good colloidal stability are efficiently functionalized with targeting units to obtain a high ratio of specific to non-specific binding.[228] To test the optimization of the bioconjugation protocol for antibody labelling of dendrimers derivatized NPs, Gubala *et al.* used different types of linkers and three generations (G0, G1 and G2) of dendrimers endowed with extensive carboxylic functionality (Fig. 15). Overall, the DDSNs-IgG (doped with the NIR-644 dye) conjugates prepared using dendrimers showed, interestingly, a significantly lower

limit of detection (LOD) and higher sensitivity than their traditional counterparts. The use of dendrimers also improved system stability and reduced aggregation. Interestingly, at low concentration of IgC, G1 showed the best results, outperforming the bigger G2 system, probably because of high steric hindrance at the NP surface in the latter case.

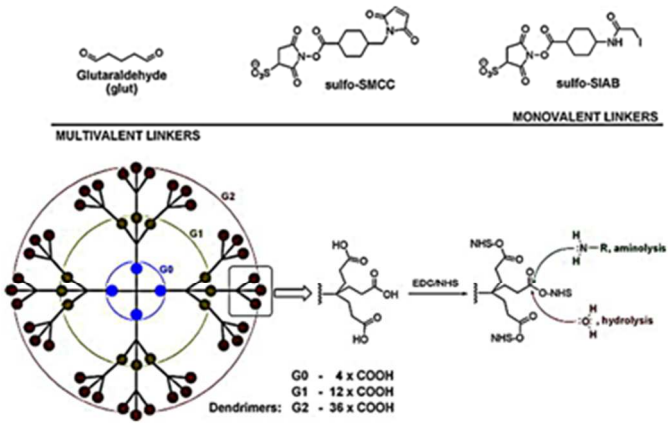


**Fig. 15** Monovalent and multivalent cross-linkers used by Gubala *et. al*.. Inset in the cartoon view of dendrimer depicting the activation of the carboxylic acids and the two competing reactions occurring on the carbonyl group. Reprinted with permission from ref. [228] Copyright 2011 Elsevier: *Talanta*.

The derivatization with dendrimers was also tested for the detection of human platelets that can be used as diagnostic tools for cardiovascular diseases.[229] In this case, the NPs doped with the NIR-644 dye were surface-coated with PAMAM dendrimers to enable efficient conjugation to platelet activation-specific antibodies (anti-CD41). The precise number of antibodies present per NP was accurately determined to optimise the platelet labelling protocol, finding that a maximum of three labelled secondary antibodies bind a single anti-CD41 primary antibody. Although the results were in favour of the high sensitivity that could be obtained using this approach, the authors underlined a problem related to the relatively low density of cell labelling, which has to be addressed to further improve analytical performance. In general, we can say that DNA microarray technology based on DDSNs can be efficiently used also for the simultaneous detection and identification of many biological contaminants and health-risk agents and, in some cases, with performances that surpass those of QDs.[230]

We find it interesting that many of the above-mentioned authors have highlighted as an additional advantage of the methodologies based on DDSNs the fact that they can be easily modified for simultaneous detection of multi-analytes. This possibility can, in fact, represent a very high added value when a rapid test is mandatory to assess the pathology of a given patient. In this context, the work proposed by the group of Tan to develop DDSNs for multiplexed bacteria monitoring and imaging[95] is extremely interesting, This approach is based on the same concept already described for distinguishing cancer cells,[184] with the possible creation of a large FRET NPs bar-coding library and can allow the diagnosis of diseases at the earliest stage of their development, by potentially eliminating the sample enrichment and amplification steps required by the current cell culture / PCR-based methods. It is important to underline that an almost complete energy transfer in similar systems has not yet been achieved. This result, when reached, could represent a very valuable feature, allowing an increase in the number of analytical approaches to detect bacteria, viruses and other pathogens.

An important frontier of modern medicine is represented by the use of therapies derived from stem cell research to potentially treat a very wide variety of diseases. In this context, tracking the distribution of stem cells *in vivo* is crucial to their therapeutic use. Traditionally, the techniques used to examine stem-cell transplantation in animal models are performed by postmortem histological analysis and consequently cannot be applied in clinical studies.[231] To noninvasively monitor the fate and distribution of transplanted stem cells, overcoming this problem, cell labelling with superparamagnetic iron oxide (SPIO) nanoparticles is now commonly used. However, stem cells lack phagocytic capacity and a transfection agent is required for sufficient internalization of SPIO NPs for cellular imaging.[232] Huang and co-workers demonstrated that nanostructures obtained by the simultaneous covering of $Fe_3O_4$@$SiO_2$ nanoparticles with mesoporous silica doped with fluorescein[233] can be conveniently used for this application. In particular, they initially determined an efficient cellular uptake of this material by human mesenchymal stem cells (hMSCs) through endocytosis, taking advantage of the bimodal (fluorescent and magnetic) nature. The procedure used to label hMSCs was reported to be fast (30 min to 1 h incubation) and the labelled cells could be visualized in a clinical 1.5-T MRI system with a minimal detectable cell number of about $10^4$ *in vitro* and with an *in vivo* detection quantity of $1.2 \times 10^5$ cells, which represents a very promising result.

The therapeutic effect of transplantation of bone marrow stem cells has been recently studied as a new therapeutic approach for advanced liver cirrhosis to avoid liver transplantation.[232] It is important to remember that liver cirrhosis, which can originate from viral hepatitis, alcohol abuse, autoimmune hepatitis and biliary disorders, leads to chronic liver failure. Kim *et al.* conveniently used for the *in vivo* visualization of transplanted stem cells commercially available fluorescent magnetic nanoparticles (MNP) containing rhodamine B within a silica shell. Although with some limitations, due to the early stage of the research, the labelling procedure used with this bimodal contrast agent has proven to be highly efficient and easy to apply, allowing the effective detection of injected stem cells in liver cirrhosis rat models.

## 5. Luminescent nanoparticles as chemosensors

The development of luminescent chemosensors for monitoring *in vitro* and *in vivo* biologically relevant analytes is a very active research field. Chemosensors can, in fact, potentially allow the investigation of the functions and possible

 

misregulation of target analytes in living systems,[234] thanks to the high sensitivity and the high spatial and temporal resolution granted by fluorescence techniques.[235-237] More and more sophisticated systems are, however, needed to address the problems of modern biology and medicine.

Together with a high signal-to-noise ratio and suitable affinity and selectivity, the ideal probe should also allow precise compartmentalization, without perturbing the equilibrium present in the cell. The risk of depleting cellular ion pools when detecting metals, for example, has been recently reported.[238] In this context, luminescent silica nanoparticles can offer interesting solutions,[55, 239, 240] overcoming many of the typical limitations of conventional chemosensors.[12, 236, 241-246]

We have already discussed some select examples of chemosensors based on luminescent DDSNs,[41] which can be used to monitor the concentration in cells, in particular of metal ions that act as biomarkers of specific diseases and/or to understand their pathogenic mechanisms. We would particularly like to stress here, together with the favourable properties that we have discussed so far, some of the unique advantages that DDSNs can offer in the field of sensing. The first is related to the possibility of properly designing collective processes such as those for energy- and electron-transfer, to obtain large signal amplifications and thus lower detection limits. Due to their collective nature, in fact, it is not possible to induce these processes in molecular probes, obtained following a supramolecular approach, with the typical fluorophore-spacer-receptor structure.[235] We have proposed a proof-of-principle of this strategy exploiting DDSNs,[247] obtained using the Stöber/Van Blaaderen methodology and doped with a chemosensor having a dansil unit as fluorophore and a polyamine as receptor.[237] In this case, thanks to a combination of photo-induced processes, we were able to demonstrate the quenching of 13 fluorescent units upon the complexation of a single copper ion, despite, due to the simple nature of the receptor, the observance of interference from Ni(II) and Co(II). In the same years, Tonellato *et al.* proposed a very elegant alternative approach to assemble, as separate subunits on the surface of silica-NPs, fluorescent dyes and receptors that resulted close enough to allow intercomponent photoinduced processes and, thus, to obtain an amplified quenching luminescence response to the presence of Cu(II) ions.[248, 249]

This method can minimize the synthetic effort, and maximize versatility, making it possible to tune the properties of these structures by adjusting the nature and ratio of the different components. However, the amplified enhancement of luminescence, i.e.: an amplified off/on chemosensor response, constitutes an even more valuable feature. To achieve this goal, very fast homo-energy transfer processes among the non-complexed moieties should be followed by very efficient hetero-energy transfer among the uncomplexed (acting as donors) and complexed units (acting as acceptors), presenting a very high fluorescent quantum yield. The above-mentioned energy transfer processes require short distances among all the different components, which can be obtained, as shown by previous results,[250] by grafting them onto the surface of the NPs. We therefore used a TSQ (a well-known probe for Zn(II) ions) derivative[251] to externally decorate and stabilize silica nanoparticles of 20 nm in diameter (Fig. 16). This system showed a 50% off/on amplified response to the presence of Zn(II). Although modest, this was the first example of amplified enhancement of the luminescence signal in nanoparticle-based chemosensors.

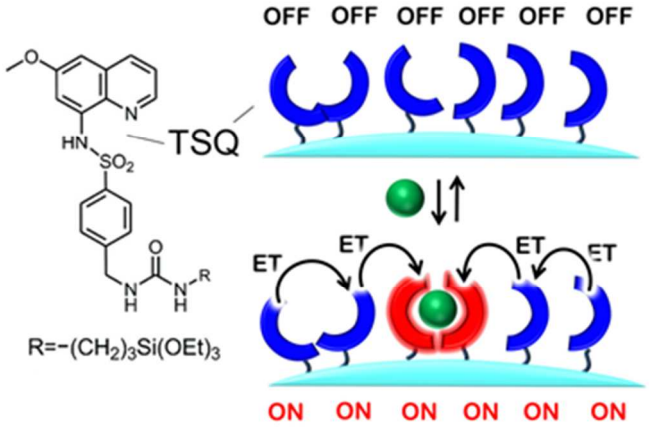


**Fig. 16** Chemical structure of the TSQ–triethoxysilane derivative (left) and schematic representation of functionalized silica nanoparticles surface (right): at low zinc concentration the excited states deactivation processes on the surfaces of the nanoparticles result in energy-transfer processes, in which the excitation energy absorbed by the surrounding free TSQ molecules is funnelled towards the fluorescent excited states. Adapted from ref. [251]. Copyright 2008 American Chemical Society.

Interestingly, the proximity of the neighbouring receptors also led to an increase in affinity toward the target analyte, a less predictable second advantage of using nanostructured probes. We obtained and observed the same two effects, namely signal amplification and affinity increase, in a different system, prepared using a non-covalent strategy, designed to monitor Cu(I) ions in biological samples where they play an important role in many physiological processes.

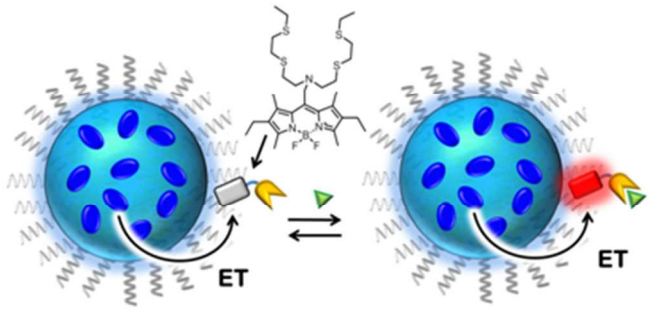


**Fig. 17** Schematic representation of the transduction mechanism in a sensing system for copper(I) ions, based on the interplay between a chemosensor and a fluorescent silica nanoparticle, to improve sensor performance at low metal ion concentrations in living cells. Adapted from ref. [120] Copyright 2011 Wiley Publishers Ltd.: *Chemistry A European Journal*.

We added to a water solution of Plus NPs doped with coumarin derivatives a bodipy-based chemosensor designed by Chang *et al.*[252] which, due to its lipophilic nature, is repartitioned

between the PEG shell of the nanostructure and the solvent (Fig. 17).[120] The chemosensor inside the polymeric layer was close enough to the nanoparticle core to enable an energy transfer process among the coumarins and the bodipy derivative. The efficiency of the energy transfer was modulated by the Cu(I) complexation, leading to a ratiometric nanosensor presenting amplification of the fluorescence response. In addition, the chemosensors inside the PEG shell showed a ten-fold increase in the association constant with Cu(I) ions, allowing a detection limit in biological environments that is lower than that attainable with the supramolecular chemosensor. A further advantage of this system is the greater separation between the excitation and emission wavelengths with respect to the molecular chemosensor, ensuring less noise. Moreover, it is important to underline a significant general advantage of using DDSNs in sensing. This strategy can, in fact, allow the use in aqueous media of otherwise water insoluble chemosensors, increasing the number of their possible applications. This is a quite general strategy as we have proved by exploiting this approach with various chemosensors for sensing Hg(II) ions in different milieu.[253, 254]

A very valuable additional advantage is represented by the possibility of inserting an analyte-independent fluorophore in the silica structure together with the fluorescent probe, leading to ratiometric systems that typically do not require calibration procedures. A very elegant system designed using this approach is represented by a nanosensor for intracellular chloride, one of the most elusive analytes in this environment, developed by Mancin *et al.* (Fig. 18).[255]

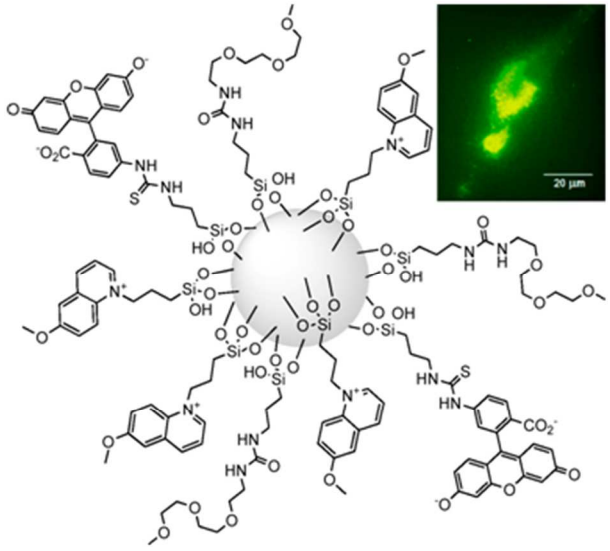


**Fig. 18** Structure of the NanoChlor assembly and fluorescence microscopy of hippocampal cells incubated with NanoChlor. Reprinted with permission from ref. [255]. Copyright 2012 American Chemical Society.

This system was obtained by grafting a probe for $Cl^-$ (a 6-methoxyquinolinium derivative), a reference dye (fluorescein) and a short poly(ethylene glycol) derivative onto the surface of commercially available silica nanoparticles to impart water solubility and to prevent nonspecific interactions with biomolecules. This properly designed system spontaneously penetrates viable cells (CHO and hippocampal cells), without showing toxicity and evidencing chemically induced chloride currents in real time.

In all the examples reported so far DDSNs were functionalized with molecular sensors; they could however also be derivatized with suitable biomolecules to increase selectivity toward a specific cellular compartment, improving the information acquirable by the system.[238] As the use of DDSNs as sensors is still in its infancy, this strategy has not yet been effectively exploited but, in our opinion, it will represent a significant research area in the near future.

The many advantages for sensing applications offered by DDSNs discussed so far can be summarized in three main concepts: versatility, modulation and multi-functionality. Their combination, which can be obtained by applying a rational and proper design, can yield the parallel optimization of many aspects of their whole performance, such as sensitivity, affinity, selectivity and internal calibration. This already makes fluorescent DDSNs unique platforms in the nanotechnology arena, although most of their potential has still to be fully developed.[12] For example, a natural implementation on which many research groups are already actively working is the multiple detection of several analytes and physical parameters, such as temperature,[256] at the same time with the same particle. The possibility of controlling a drug delivery process (which is, as we have already discussed, a possible function of silica nanoparticles) to the concentration of the detected biologically relevant analyte represents a very attractive, although difficult, goal that can be reached only in a long-term perspective.

## 6. Conclusions

Luminescent silica nanoparticles, which supply increased chemical stability to the loaded species also under different external stimuli and present unique physiochemical features, find a wide range of possible applications in the medical field. Tuneable optical properties and facile size/shape/surface modifications, make DDSNs versatile multifunctional platforms for imaging, drug delivery, and theranostics. They represent an excellent tool for fundamental research and a great promise for extensive translation to clinical practice. However, before this can occur, their accumulation and potential long-term toxicity have to be understood.

New standardized and dedicated test methods are needed to evaluate the possible toxic effects and potential risks associated with nanoparticles. At present, to address the problem of long-term stability, great effort is being devoted to the investigation of surface functionalization, which should also be able to provide bioactive interfaces. We hope that the data discussed in this review article can hekp highlight the amount of progress that has already been made in this direction, with promising results for more and more ambitious goals.

Progress in the engineering of multifunctional silica NPs, in fact, represents one of the most encouraging outcomes toward

 

the development of theranostic nanomedicine, improving early diagnosis but also the safety and efficacy of therapy.

At present, most nanomedicine-based drug/dye delivery systems are still in the preclinical development stage but we are very optimistic that the start of the clinical trials could be very near. Although not exhaustive, the currently available data favours the benign nature of DDSNs and this allows us to envisage a successful acceleration of translational research in the next few years.

## Acknowledgements

We would like to thank the Italian Ministry of University and Research MIUR (PRIN 2009Z9ASCA and PON 01_01078 projects), and University of Bologna (FARB project) for their funding.

## Notes and references

[a] Department of Chemistry "G. Ciamician", University of Bologna, Via Selmi 2, 40126 Bologna, Italy.

1. J. Oeppen and J. W. Vaupel, *Science*, 2002, **296**, 1029-1031.
2. S. Kaur, G. Venktaraman, M. Jain, S. Senapati, P. K. Garg and S. K. Batra, *Cancer Lett.*, 2012, **315**, 97-111.
3. R. L. Buckner, F. M. Krienen and B. T. T. Yeo, *Nat. Neurosci.*, 2013, **16**, 832-837.
4. M. De, S. S. Chou, H. M. Joshi and V. P. Dravid, *Adv. Drug Del. Rev.*, 2011, **63**, 1282-1299.
5. N. C. Cowan, *Nat. Rev. Urol.*, 2012, **9**, 218-226.
6. K. Chen and P. S. Conti, *Adv. Drug Del. Rev.*, 2010, **62**, 1005-1022.
7. H. Jaffer, I. M. Adjei and V. Labhasetwar, *Sci. Rep.*, 2013, **3**.
8. A. L. Vahrmeijer, M. Hutteman, J. R. van der Vorst, C. J. H. van de Velde and J. V. Frangioni, *Nat. Rev. Clin. Oncol.*, 2013, **10**, 507-518.
9. M. Hecht, E. Climent, M. Biyikal, F. Sancenón, R. Martínez-Máñez and K. Rurack, *Coord. Chem. Rev.*, 2013, **257**, 2589-2606.
10. J. Kim, Y. Piao and T. Hyeon, *Chem. Soc. Rev.*, 2009, **38**, 372-390.
11. P. N. Prasad, *Introduction to Nanomedicine and Nanobioengineering*, John Wiley & Sons, 2012.
12. S. Bonacchi, D. Genovese, R. Juris, M. Montalti, L. Prodi, E. Rampazzo and N. Zaccheroni, *Angew. Chem. Int. Ed.*, 2011, **50**, 4056-4066.
13. S. Bonacchi, D. Genovese, R. Juris, M. Montalti, L. Prodi, E. Rampazzo, M. Sgarzi and N. Zaccheroni, in *Luminescence Applied in Sensor Science*, eds. L. Prodi, M. Montalti and N. Zaccheroni, Springer Berlin Heidelberg, 2011, **vol. 300**, ch. 104, pp. 93-138.
14. F. Puntoriero, F. Nastasi, M. Cavazzini, S. Quici and S. Campagna, *Coord. Chem. Rev.*, 2007, **251**, 536-545.
15. S. Bonacchi, D. Genovese, R. Juris, E. Marzocchi, M. Montalti, L. Prodi, E. Rampazzo and N. Zaccheroni, in *Reviews in Fluorescence 2008*, ed. C. Geddes, Springer New York, 2010, **vol. 2008**, ch. 5, pp. 119-137.
16. J.-M. Lehn, *Angew. Chem. Int. Ed.*, 2013, **52**, 2836-2850.
17. E. Rampazzo, S. Bonacchi, R. Juris, M. Montalti, D. Genovese, N. Zaccheroni, L. Prodi, D. C. Rambaldi, A. Zattoni and P. Reschiglian, *J. Phys. Chem. B*, 2010, **114**, 14605-14613.
18. D. Genovese, S. Bonacchi, R. Juris, M. Montalti, L. Prodi, E. Rampazzo and N. Zaccheroni, *Angew. Chem. Int. Ed.*, 2013, **52**, 5965-5968.
19. L. S. Dolci, S. Zanarini, L. D. Ciana, F. Paolucci and A. Roda, *Anal. Chem.*, 2009, **81**, 6234-6241.
20. A. Roda, M. Di Fusco, A. Quintavalla, M. Guardigli, M. Mirasoli, M. Lombardo and C. Trombini, *Anal. Chem.*, 2012, **84**, 9913-9919.
21. G. Valenti, E. Rampazzo, S. Bonacchi, T. Khajvand, R. Juris, M. Montalti, M. Marcaccio, F. Paolucci and L. Prodi, *Chem. Commun.*, 2012, **48**, 4187-4189.
22. E. Rampazzo, S. Bonacchi, D. Genovese, R. Juris, M. Marcaccio, M. Montalti, F. Paolucci, M. Sgarzi, G. Valenti, N. Zaccheroni and L. Prodi, *Coord. Chem. Rev.*, 2012, **256**, 1664-1681.
23. S. W. Bae, W. Tan and J.-I. Hong, *Chem. Commun.*, 2012, **48**, 2270-2282.
24. M. S. Bradbury, E. Phillips, P. H. Montero, S. M. Cheal, H. Stambuk, J. C. Durack, C. T. Sofocleous, R. J. C. Meester, U. Wiesner and S. Patel, *Integr. Biol.*, 2013, **5**, 74-86.
25. P. C. Ray, S. A. Khan, A. K. Singh, D. Senapati and Z. Fan, *Chem. Soc. Rev.*, 2012, **41**, 3193-3209.
26. W. Arap, R. Pasqualini, M. Montalti, L. Petrizza, L. Prodi, E. Rampazzo, N. Zaccheroni and S. Marchio, *Curr. Med. Chem.*, 2013, **20**, 2195-2211.
27. M. Miragoli, P. Novak, P. Ruenraroengsak, A. I. Shevchuk, Y. E. Korchev, M. J. Lab, T. D. Tetley and J. Gorelik, *Nanomedicine*, 2012, **8**, 725-737.
28. S. Prilloff, J. Fan, P. Henrich-Noack and B. A. Sabel, *Eur. J. Neurosci.*, 2010, **31**, 521-528.
29. F. Novio, J. Simmchen, N. Vázquez-Mera, L. Amorín-Ferré and D. Ruiz-Molina, *Coord. Chem. Rev.*, 2013, **257**, 2839-2847.
30. P. Wu and X.-P. Yan, *Chem. Soc. Rev.*, 2013, **42**, 5489-5521.
31. V. Lesnyak, N. Gaponik and A. Eychmuller, *Chem. Soc. Rev.*, 2013, **42**, 2905-2929.
32. A. Taylor, K. M. Wilson, P. Murray, D. G. Fernig and R. Levy, *Chem. Soc. Rev.*, 2012, **41**, 2707-2717.
33. R. Freeman, J. Girsh and I. Willner, *ACS Appl. Mater. Inter.*, 2013, **5**, 2815-2834.
34. R. Freeman, B. Willner and I. Willner, *J. Phys. Chem. Lett.*, 2011, **2**, 2667-2677.
35. I. Willner and B. Willner, *Nano Lett.*, 2010, **10**, 3805-3815.
36. M. Amelia, C. Lincheneau, S. Silvi and A. Credi, *Chem. Soc. Rev.*, 2012, **41**, 5728-5743.
37. E. Margapoti, D. Gentili, M. Amelia, A. Credi, V. Morandi and M. Cavallini, *Nanoscale*, 2013.
38. A. Credi, *New J. Chem.*, 2012, **36**, 1925-1930.
39. Y. Wang, R. Hu, G. Lin, I. Roy and K.-T. Yong, *ACS Appl. Mater. Inter.*, 2013, **5**, 2786-2799.
40. Y. Piao, A. Burns, J. Kim, U. Wiesner and T. Hyeon, *Adv. Funct. Mater.*, 2008, **18**, 3745-3758.
41. M. Montalti, E. Rampazzo, N. Zaccheroni and L. Prodi, *New J. Chem.*, 2013, **37**, 28-34.

42. M. Helle, E. Rampazzo, M. Monchanin, F. Marchal, F. Guillemin, S. Bonacchi, F. Salis, L. Prodi and L. Bezdetnaya, *ACS Nano*, 2013, **7**, 8645-8657.
43. R. Kumar, I. Roy, T. Y. Ohulchanskyy, L. N. Goswami, A. C. Bonoiu, E. J. Bergey, K. M. Tramposch, A. Maitra and P. N. Prasad, *ACS Nano*, 2008, **2**, 449-456.
44. J. L. Vivero-Escoto, R. C. Huxford-Phillips and W. Lin, *Chem. Soc. Rev.*, 2012, **41**, 2673-2685.
45. M. A. Rocco, J.-Y. Kim, A. Burns, J. Kostecki, A. Doody, U. Wiesner and M. P. DeLisa, *Bioconj. Chem.*, 2009, **20**, 1482-1489.
46. M. Soster, R. Juris, S. Bonacchi, D. Genovese, M. Montalti, E. Rampazzo, N. Zaccheroni, P. Garagnani, F. Bussolino, L. Prodi and S. Marchio, *Int. J. Nanomed.*, 2012, **7**, 4797-4807.
47. J. H. Ryu, H. Koo, I.-C. Sun, S. H. Yuk, K. Choi, K. Kim and I. C. Kwon, *Adv. Drug Del. Rev.*, 2012, **64**, 1447-1458.
48. S. Dufort, L. Sancey and J.-L. Coll, *Adv. Drug Del. Rev.*, 2012, **64**, 179-189.
49. S. Bonacchi, D. Genovese, R. Juris, M. Montalti, L. Prodi, E. Rampazzo, M. Sgarzi and N. Zaccheroni, *Top. Curr. Chem.*, 2011, **300**, 93-138.
50. A. Burns, P. Sengupta, T. Zedayko, B. Baird and U. Wiesner, *Small*, 2006, **2**, 723-726.
51. R. I. Nooney, E. McCormack and C. McDonagh, *Anal. Bioanal. Chem.*, 2012, **404**, 2807-2818.
52. L. Wang and W. Tan, *Nano Lett.*, 2005, **6**, 84-88.
53. J. Yan, M. C. Estévez, J. E. Smith, K. Wang, X. He, L. Wang and W. Tan, *Nano Today*, 2007, **2**, 44-50.
54. D. Genovese, E. Rampazzo, S. Bonacchi, M. Montalti, N. zaccheroni and L. Prodi, *Nanoscale*, 2013, DOI: 10.1039/c1033nr05599j.
55. T. Doussineau, A. Schulz, A. Lapresta-Fernandez, A. Moro, S. Korsten, S. Trupp and G. J. Mohr, *Chem. Eur. J.*, 2010, **16**, 10290-10299.
56. M. Arduini, F. Mancin, P. Tecilla and U. Tonellato, *Langmuir*, 2007, **23**, 8632-8636.
57. L. Wang, M. B. O'Donoghue and W. Tan, *Nanomedicine (Lond)*, 2006, **1**, 413-426.
58. S. Sharifi, S. Behzadi, S. Laurent, M. Laird Forrest, P. Stroeve and M. Mahmoudi, *Chem. Soc. Rev.*, 2012, **41**, 2323-2343.
59. K. E. Sapsford, W. R. Algar, L. Berti, K. B. Gemmill, B. J. Casey, E. Oh, M. H. Stewart and I. L. Medintz, *Chem. Rev.*, 2013, **113**, 1904-2074.
60. N. Lewinski, V. Colvin and R. Drezek, *Small*, 2008, **4**, 26-49.
61. B. Halamoda Kenzaoui, C. Chapuis Bernasconi, S. Guney-Ayra and L. Juillerat-Jeanneret, *Biochem. J.*, 2012, **441**, 813-821.
62. H. C. Fischer and W. C. W. Chan, *Curr. Opin. Biotechnol.*, 2007, **18**, 565-571.
63. N. Khlebtsov and L. Dykman, *Chem Soc Rev*, 2011, **40**, 1647-1671.
64. M. Mahmoudi, H. Hofmann, B. Rothen-Rutishauser and A. Petri-Fink, *Chem. Rev.*, 2012, **112**, 2323-2338.
65. E. Rampazzo, R. Voltan, L. Petrizza, N. Zaccheroni, L. Prodi, F. Casciano, G. Zauli and P. Secchiero, *Nanoscale*, 2013, **5**, 7897-7905.
66. X. He, H. Nie, K. Wang, W. Tan, X. Wu and P. Zhang, *Anal. Chem.*, 2008, **80**, 9597-9603.
67. A. A. Burns, J. Vider, H. Ow, E. Herz, O. Penate-Medina, M. Baumgart, S. M. Larson, U. Wiesner and M. Bradbury, *Nano Lett.*, 2008, **9**, 442-448.
68. K.-T. Yong, W.-C. Law, R. Hu, L. Ye, L. Liu, M. T. Swihart and P. N. Prasad, *Chem. Soc. Rev.*, 2013, **42**, 1236-1250.
69. D. Tarn, C. E. Ashley, M. Xue, E. C. Carnes, J. I. Zink and C. J. Brinker, *Acc. Chem. Res.*, 2013, **46**, 792-801.
70. S. Mura and P. Couvreur, *Adv. Drug Del. Rev.*, 2012, **64**, 1394-1416.
71. A. L. Petersen, A. E. Hansen, A. Gabizon and T. L. Andresen, *Adv. Drug Del. Rev.*, 2012, **64**, 1417-1435.
72. R. Bardhan, S. Lal, A. Joshi and N. J. Halas, *Acc. Chem. Res.*, 2011, **44**, 936-946.
73. Y. Chen, H. Chen and J. Shi, *Adv. Mater.*, 2013, **25**, 3144-3176.
74. J. E. Lee, N. Lee, T. Kim, J. Kim and T. Hyeon, *Acc. Chem. Res.*, 2011, **44**, 893-902.
75. Z. Li, J. C. Barnes, A. Bosoy, J. F. Stoddart and J. I. Zink, *Chem. Soc. Rev.*, 2012, **41**, 2590-2605.
76. L. L. Hench and J. K. West, *Chem. Rev.*, 1990, **90**, 33-72.
77. S. Zanarini, E. Rampazzo, L. D. Ciana, M. Marcaccio, E. Marzocchi, M. Montalti, F. Paolucci and L. Prodi, *J. Am. Chem. Soc.*, 2009, **131**, 2260-2267.
78. R. P. Bagwe, C. Yang, L. R. Hilliard and W. Tan, *Langmuir*, 2004, **20**, 8336-8342.
79. S. Zanarini, E. Rampazzo, S. Bonacchi, R. Juris, M. Marcaccio, M. Montalti, F. Paolucci and L. Prodi, *J. Am. Chem. Soc.*, 2009, **131**, 14208-14209.
80. K. T. Yong, I. Roy, M. T. Swihart and P. N. Prasad, *J. Mater. Chem.*, 2009, **19**, 4655-4672.
81. A. Van Blaaderen, A. Imhof, W. Hage and A. Vrij, *Langmuir*, 1992, **8**, 1514-1517.
82. N. A. M. Verhaegh and A. v. Blaaderen, *Langmuir*, 1994, **10**, 1427-1438.
83. G. Kolbe, 1956.
84. W. Stöber, A. Fink and E. Bohn, *J. Colloid Interface Sci.*, 1968, **26**, 62-69.
85. A. Van Blaaderen and A. Vrij, *Langmuir*, 1992, **8**, 2921-2931.
86. E. Rampazzo, S. Bonacchi, M. Montalti, L. Prodi and N. Zaccheroni, *J. Am. Chem. Soc.*, 2007, **129**, 14251-14256.
87. J. Wang, A. Sugawara-Narutaki, M. Fukao, T. Yokoi, A. Shimojima and T. Okubo, *ACS Appl. Mater. Inter.*, 2011, **3**, 1538-1544.
88. R. Nyffenegger, C. Quellet and J. Ricka, *J. Colloid Interface Sci.*, 1993, **159**, 150-157.
89. H. Ow, D. R. Larson, M. Srivastava, B. A. Baird, W. W. Webb and U. Wiesner, *Nano Lett.*, 2004, **5**, 113-117.
90. D. R. Larson, H. Ow, H. D. Vishwasrao, A. A. Heikal, U. Wiesner and W. W. Webb, *Chem. Mater.*, 2008, **20**, 2677-2684.
91. M. Montalti, L. Prodi, N. Zaccheroni, A. Zattoni, P. Reschiglian and G. Falini, *Langmuir*, 2004, **20**, 2989-2991.
92. R. P. Bagwe, L. R. Hilliard and W. Tan, *Langmuir*, 2006, **22**, 4357-4362.
93. F. J. Arriagada and K. Osseo-Asare, *J. Colloid Interface Sci.*, 1995, **170**, 8-17.
94. L. Wang, C. Lofton, M. Popp and W. Tan, *Bioconj. Chem.*, 2007, **18**, 610-613.

 

95. L. Wang, W. Zhao, M. B. O'Donoghu and W. Tan, *Bioconj. Chem.*, 2007, **18**, 297-301.
96. C.-L. Chang and H. S. Fogler, *Langmuir*, 1997, **13**, 3295-3307.
97. S. Kim, H. Huang, H. E. Pudavar, Y. Cui and P. N. Prasad, *Chem. Mater.*, 2007, **19**, 5650-5656.
98. S. Kim, T. Y. Ohulchanskyy, H. E. Pudavar, R. K. Pandey and P. N. Prasad, *J. Am. Chem. Soc.*, 2007, **129**, 2669-2675.
99. I. Roy, T. Y. Ohulchanskyy, H. E. Pudavar, E. J. Bergey, A. R. Oseroff, J. Morgan, T. J. Dougherty and P. N. Prasad, *J. Am. Chem. Soc.*, 2003, **125**, 7860-7865.
100. C. Compagnin, L. Bau, M. Mognato, L. Celotti, G. Miotto, M. Arduini, F. Moret, C. Fede, F. Selvestrel, I. M. R. Echevarria, F. Mancin and E. Reddi, *Nanotechnology*, 2009, **20**.
101. T. Y. Ohulchanskyy, I. Roy, L. N. Goswami, Y. Chen, E. J. Bergey, R. K. Pandey, A. R. Oseroff and P. N. Prasad, *Nano Lett.*, 2007, **7**, 2835-2842.
102. F. Selvestrel, F. Moret, D. Segat, J. H. Woodhams, G. Fracasso, I. M. R. Echevarria, L. Bau, F. Rastrelli, C. Compagnin, E. Reddi, C. Fedeli, E. Papini, R. Tavano, A. Mackenzie, M. Bovis, E. Yaghini, A. J. MacRobert, S. Zanini, A. Boscaini, M. Colombatti and F. Mancin, *Nanoscale*, 2013, **5**, 6106-6116.
103. I. Roy, T. Y. Ohulchanskyy, D. J. Bharali, H. E. Pudavar, R. A. Mistretta, N. Kaur and P. N. Prasad, *Proc. Natl. Acad. Sci. U. S. A.*, 2005, **102**, 279-284.
104. D. J. Bharali, I. Klejbor, E. K. Stachowiak, P. Dutta, I. Roy, N. Kaur, E. J. Bergey, P. N. Prasad and M. K. Stachowiak, *Proc. Natl. Acad. Sci. U. S. A.*, 2005, **102**, 11539-11544.
105. R. Kumar, I. Roy, T. Y. Ohulchanskky, L. A. Vathy, E. J. Bergey, M. Sajjad and P. N. Prasad, *ACS Nano*, 2010, **4**, 699-708.
106. A. Seddon and D. Li Ou, *J. Sol-Gel Sci. Technol.*, 1998, **13**, 623-628.
107. W.-C. Law, K.-T. Yong, I. Roy, G. Xu, H. Ding, E. J. Bergey, H. Zeng and P. N. Prasad, *J. Phys. Chem. C*, 2008, **112**, 7972-7977.
108. K. Ma, U. Werner-Zwanziger, J. Zwanziger and U. Wiesner, *Chem. Mater.*, 2013, **25**, 677-691.
109. K. Ma, H. Sai and U. Wiesner, *J. Am. Chem. Soc.*, 2012, **134**, 13180-13183.
110. Q. Huo, J. Liu, L.-Q. Wang, Y. Jiang, T. N. Lambert and E. Fang, *J. Am. Chem. Soc.*, 2006, **128**, 6447-6453.
111. F. Chi, B. Guan, B. Yang, Y. Liu and Q. Huo, *Langmuir*, 2010, **26**, 11421-11426.
112. F. Chi, Y.-N. Guo, J. Liu, Y. Liu and Q. Huo, *J. Phys. Chem. C*, 2010, **114**, 2519-2523.
113. J. Liu, S. Bai, H. Zhong, C. Li and Q. Yang, *J. Phys. Chem. C*, 2009, **114**, 953-961.
114. M. Mandal and M. Kruk, *Chem. Mater.*, 2011, **24**, 123-132.
115. E. Rampazzo, F. Boschi, S. Bonacchi, R. Juris, M. Montalti, N. Zaccheroni, L. Prodi, L. Calderan, B. Rossi, S. Becchi and A. Sbarbati, *Nanoscale*, 2012, **4**, 824-830.
116. B. L. Cushing, V. L. Kolesnichenko and C. J. O'Connor, *Chem. Rev.*, 2004, **104**, 3893-3946.
117. D. Gallagher and T. A. Ring, *Chimia*, 1989, **43**, 298.
118. P. R. Desai, N. J. Jain, R. K. Sharma and P. Bahadur, *Colloids Surf. Physicochem. Eng. Aspects*, 2001, **178**, 57-69.
119. A. Pedone, E. Gambuzzi, V. Barone, S. Bonacchi, D. Genovese, E. Rampazzo, L. Prodi and M. Montalti, *PCCP*, 2013, **15**, 12360-12372.
120. E. Rampazzo, S. Bonacchi, D. Genovese, R. Juris, M. Sgarzi, M. Montalti, L. Prodi, N. Zaccheroni, G. Tomaselli, S. Gentile, C. Satriano and E. Rizzarelli, *Chemistry – A European Journal*, 2011, **17**, 13429-13432.
121. D. Genovese, M. Montalti, L. Prodi, E. Rampazzo, N. Zaccheroni, O. Tosic, K. Altenhoner, F. May and J. Mattay, *Chem. Commun.*, 2011, **47**, 10975-10977.
122. X.-d. Wang, J. A. Stolwijk, T. Lang, M. Sperber, R. J. Meier, J. Wegener and O. S. Wolfbeis, *J. Am. Chem. Soc.*, 2012, **134**, 17011-17014.
123. K. E. Sapsford, W. R. Algar, L. Berti, K. B. Gemmill, B. J. Casey, E. Oh, M. H. Stewart and I. L. Medintz, *Chem. Rev. (Washington, DC, U. S.)*, 2013, **113**, 1904-2074.
124. W. R. Algar, D. E. Prasuhn, M. H. Stewart, T. L. Jennings, J. B. Blanco-Canosa, P. E. Dawson and I. L. Medintz, *Bioconjugate Chem.*, 2011, **22**, 825-858.
125. L. Yang, X. Zhang, M. Ye, J. Jiang, R. Yang, T. Fu, Y. Chen, K. Wang, C. Liu and W. Tan, *Adv. Drug Delivery Rev.*, 2011, **63**, 1361-1370.
126. A. Aravind, Y. Yoshida, T. Maekawa and D. S. Kumar, *Drug Delivery Transl. Res.*, 2012, **2**, 418-436.
127. M. M. Di, S. Shamsuddin, R. K. Abdul, A. A. Abdul, C. Devaux, E. Borghi, L. Levy and C. Sadun, *Int. J. Nanomed.*, 2010, **5**, 37-49.
128. R. A. Sperling and W. J. Parak, *Philosophical Transactions of the Royal Society A: Mathematical, Physical and Engineering Sciences*, 2010, **368**, 1333-1383.
129. N. Erathodiyil and J. Y. Ying, *Acc. Chem. Res.*, 2011, **44**, 925-935.
130. A. M. Smith, H. Duan, A. M. Mohs and S. Nie, *Adv. Drug Delivery Rev.*, 2008, **60**, 1226-1240.
131. V. Biju, S. Mundayoor, R. V. Omkumar, A. Anas and M. Ishikawa, *Biotechnol. Adv.*, 2010, **28**, 199-213.
132. M. F. Frasco and N. Chaniotakis, *Anal. Bioanal. Chem.*, 2010, **396**, 229-240.
133. N. Vijayasree, K. Haritha, V. Subhash and K. R. S. S. Rao, *Res. J. BioTechnol.*, 2009, **4**, 61-66.
134. J. E. Smith, L. Wang and W. Tan, *TrAC, Trends Anal. Chem.*, 2006, **25**, 848-855.
135. W. Tan, K. Wang, X. He, X. J. Zhao, T. Drake, L. Wang and R. P. Bagwe, *Med. Res. Rev.*, 2004, **24**, 621-638.
136. L. Wang, W. Zhao and W. Tan, *Nano Res.*, 2008, **1**, 99-115.
137. K. Paulkumar, R. Arunachalam and G. Annadurai, *Int. J. Nanotechnol.*, 2011, **8**, 653-663.
138. L. Wang, K. Wang, S. Santra, X. Zhao, L. R. Hilliard, J. E. Smith, Y. Wu and W. Tan, *Anal. Chem.*, 2006, **78**, 646-654.
139. C. Rocker, M. Potzl, F. Zhang, W. J. Parak and G. U. Nienhaus, *Nature Nanotechnology*, 2009, **4**, 577-580.
140. M. P. Monopoli, C. Aberg, A. Salvati and K. A. Dawson, *Nature Nanotechnology*, 2012, **7**, 779-786.
141. M. Mahmoudi, S. N. Saeedi-Eslami, M. A. Shokrgozar, K. Azadmanesh, M. Hassanlou, H. R. Kalhor, C. Burtea, B. Rothen-Rutishauser, S. Laurent, S. Sheibani and H. Vali, *Nanoscale*, 2012, **4**, 5461-5468.

142. M. P. Monopoli, D. Walczyk, A. Campbell, G. Elia, I. Lynch, B. F. Baldelli and K. A. Dawson, *J. Am. Chem. Soc.*, 2011, **133**, 2525-2534.
143. M. Mahmoudi, I. Lynch, M. R. Ejtehadi, M. P. Monopoli, F. B. Bombelli and S. Laurent, *Chemical Reviews*, 2011, **111**, 5610-5637.
144. T. Cedervall, I. Lynch, S. Lindman, T. Berggård, E. Thulin, H. Nilsson, K. A. Dawson and S. Linse, *Proceedings of the National Academy of Sciences*, 2007, **104**, 2050-2055.
145. C. H. Yu, A. Al-Saadi, S.-J. Shih, L. Qiu, K. Y. Tam and S. C. Tsang, *The Journal of Physical Chemistry C*, 2008, **113**, 537-543.
146. J. S. Gebauer, M. Malissek, S. Simon, S. K. Knauer, M. Maskos, R. H. Stauber, W. Peukert and L. Treuel, *Langmuir*, 2012, **28**, 9673-9679.
147. A. M. Moulin, S. J. O'Shea, R. A. Badley, P. Doyle and M. E. Welland, *Langmuir*, 1999, **15**, 8776-8779.
148. Y. Yan, G. K. Such, A. P. R. Johnston, H. Lomas and F. Caruso, *ACS Nano*, 2011, **5**, 4252-4257.
149. A. L. Becker, A. P. R. Johnston and F. Caruso, *Small*, 2010, **6**, n/a-n/a.
150. T. Xia, M. Kovochich, M. Liong, H. Meng, S. Kabehie, S. George, J. I. Zink and A. E. Nel, *ACS Nano*, 2009, **3**, 3273-3286.
151. W.-T. He, Y.-N. Xue, N. Peng, W.-M. Liu, R.-X. Zhuo and S.-W. Huang, *J. Mater. Chem.*, 2011, **21**, 10496-10503.
152. C. Haensch, S. Hoeppener and U. S. Schubert, *Chem. Soc. Rev.*, 2010, **39**, 2323-2334.
153. D. Gerion, F. Pinaud, S. C. Williams, W. J. Parak, D. Zanchet, S. Weiss and A. P. Alivisatos, *The Journal of Physical Chemistry B*, 2001, **105**, 8861-8871.
154. S. Santra, R. Tapec, N. Theodoropoulou, J. Dobson, A. Hebard and W. Tan, *Langmuir*, 2001, **17**, 2900-2906.
155. S. Liu and M.-Y. Han, *Chemistry – An Asian Journal*, 2010, **5**, 36-45.
156. Y. An, M. Chen, Q. Xue and W. Liu, *J. Colloid Interface Sci.*, 2007, **311**, 507-513.
157. C. Kneuer, M. Sameti, U. Bakowsky, T. Schiestel, H. Schirra, H. Schmidt and C.-M. Lehr, *Bioconj. Chem.*, 2000, **11**, 926-932.
158. L. Han, Y. Sakamoto, O. Terasaki, Y. Li and S. Che, *J. Mater. Chem.*, 2007, **17**, 1216-1221.
159. Y. Wu, C. Chen and S. Liu, *Anal. Chem.*, 2009, **81**, 1600-1607.
160. R. Voss, M. A. Brook, J. Thompson, Y. Chen, R. H. Pelton and J. D. Brennan, *J. Mater. Chem.*, 2007, **17**, 4854-4863.
161. J. Kobler, K. Möller and T. Bein, *ACS Nano*, 2008, **2**, 791-799.
162. M. Nakamura and K. Ishimura, *The Journal of Physical Chemistry C*, 2007, **111**, 18892-18898.
163. M. Nakamura and K. Ishimura, *Langmuir*, 2008, **24**, 5099-5108.
164. M. Soster, R. Juris, S. Bonacchi, D. Genovese, M. Montalti, E. Rampazzo, N. Zaccheroni, P. Garagnani, F. Bussolino, L. Prodi and S. Marchio, *International Journal of Nanomedicine*, 2012, **7**, 4797-4807.
165. R. P. Haugland, *The Handbook A Guide to Fluorescent Probes and Labeling Technologies*, Invitrogen, San Diego, 10th ed. edn., 2005.
166. G. T. Hermanson, *Bioconjugate Techniques*, Academic Press, San Diego, 2nd ed. edn., 2008.
167. H. C. Kolb, M. G. Finn and K. B. Sharpless, *Angew. Chem. Int. Ed.*, 2001, **40**, 2004-2021.
168. D. E. Achatz, F. J. Heiligtag, X. Li, M. Link and O. S. Wolfbeis, *Sensors Actuators B: Chem.*, 2010, **150**, 211-219.
169. C. Chen, J. Geng, F. Pu, X. Yang, J. Ren and X. Qu, *Angew. Chem. Int. Ed.*, 2011, **50**, 882-886.
170. K. Patel, S. Angelos, W. R. Dichtel, A. Coskun, Y.-W. Yang, J. I. Zink and J. F. Stoddart, *J. Am. Chem. Soc.*, 2008, **130**, 2382-2383.
171. M. Howarth, K. Takao, Y. Hayashi and A. Y. Ting, *Proc. Natl. Acad. Sci. U. S. A.*, 2005, **102**, 7583-7588.
172. I. Chen, Y.-A. Choi and A. Y. Ting, *J. Am. Chem. Soc.*, 2007, **129**, 6619-6625.
173. Z. Xia, Y. Xing, M.-K. So, A. L. Koh, R. Sinclair and J. Rao, *Anal. Chem.*, 2008, **80**, 8649-8655.
174. D. R. Elias, Z. Cheng and A. Tsourkas, *Small*, 2010, **6**, 2460-2468.
175. D. Liße, V. Wilkens, C. You, K. Busch and J. Piehler, *Angew. Chem. Int. Ed.*, 2011, **50**, 9352-9355.
176. Y. Zhang, M.-k. So, A. M. Loening, H. Yao, S. S. Gambhir and J. Rao, *Angew. Chem. Int. Ed.*, 2006, **45**, 4936-4940.
177. M. Muellner, A. Schallon, A. Walther, R. Freitag and A. H. E. Mueller, *Biomacromolecules*, 2010, **11**, 390-396.
178. J. S. Brodbelt, *J. Am. Chem. Soc.*, 2009, **131**, 11635-11636.
179. M. Famulok, J. S. Hartig and G. Mayer, *Chem. Rev.*, 2007, **107**, 3715-3743.
180. W. Tan, M. J. Donovan and J. Jiang, *Chem. Rev.*, 2013, **113**, 2842-2862.
181. L. Cai, Z.-Z. Chen, M.-Y. Chen, H.-W. Tang and D.-W. Pang, *Biomaterials*, 2013, **34**, 371-381.
182. F. Cao, R. Deng, D. Liu, S. Song, S. Wang, S. Su and H. Zhang, *Dalton Trans.*, 2011, **40**, 4800-4802.
183. J. E. Smith, C. D. Medley, Z. Tang, D. Shangguan, C. Lofton and W. Tan, *Anal. Chem.*, 2007, **79**, 3075-3082.
184. X. Chen, M. C. Estevez, Z. Zhu, Y.-F. Huang, Y. Chen, L. Wang and W. Tan, *Anal. Chem.*, 2009, **81**, 7009-7014.
185. Z.-Z. Chen, L. Cai, X.-M. Dong, H.-W. Tang and D.-W. Pang, *Biosensors Bioelectron.*, 2012, **37**, 75-81.
186. X. Song, F. Li, J. Ma, N. Jia, J. Xu and H. Shen, *J. Fluoresc.*, 2011, **21**, 1205-1212.
187. S. Huang, R. Li, Y. Qu, J. Shen and J. Liu, *J. Fluoresc.*, 2009, **19**, 1095-1101.
188. X. Wang, A. R. Morales, T. Urakami, L. Zhang, M. V. Bondar, M. Komatsu and K. D. Belfield, *Bioconj. Chem.*, 2011, **22**, 1438-1450.
189. W. Yanli, X. Xianzhu, T. Qun and L. Yongxiu, *Nanotechnology*, 2012, **23**, 205103.
190. H. Tan, M. Wang, C. T. Yang, S. Pant, K. K. Bhakoo, S. Y. Wong, Z. K. Chen, X. Li and J. Wang, *Chemistry – A European Journal*, 2011, **17**, 6696-6706.
191. F. Corsi, C. De Palma, M. Colombo, R. Allevi, M. Nebuloni, S. Ronchi, G. Rizzi, A. Tosoni, E. Trabucchi, E. Clementi and D. Prosperi, *Small*, 2009, **5**, 2555-2564.
192. D. Niu, Y. Li, Z. Ma, H. Diao, J. Gu, H. Chen, W. Zhao, M. Ruan, Y. Zhang and J. Shi, *Adv. Funct. Mater.*, 2010, **20**, 773-780.
193. A. Bumb, C. A. S. Regino, M. R. Perkins, M. Bernardo, M. Ogawa, L. Fugger, P. L. Choyke, P. J. Dobson and M. W. Brechbiel, *Nanotechnology*, 2010, **21**, 175704-175704.
194. J. S. Kim, Y. H. Kim, J. H. Kim, K. W. Kang, E. L. Tae, H. Youn, D. Kim, S. K. Kim, J. T. Kwon, M. H. Cho, Y. S. Lee, J. M. Jeong, J. K. Chung and D. S. Lee, *Nanomedicine*, 2012, **7**, 219-229.

 

195. T. Luo, P. Huang, G. Gao, G. Shen, S. Fu, D. Cui, C. Zhou and Q. Ren, *Opt. Express*, 2011, **19**, 17030-17039.
196. L. Wang, K. G. Neoh, E. T. Kang and B. Shuter, *Biomaterials*, 2011, **32**, 2166-2173.
197. H. Yang, Y. Zhuang, H. Hu, X. Du, C. Zhang, X. Shi, H. Wu and S. Yang, *Adv. Funct. Mater.*, 2010, **20**, 1733-1741.
198. Y.-S. Cho, T.-J. Yoon, E.-S. Jang, K. Soo Hong, S. Young Lee, O. Ran Kim, C. Park, Y.-J. Kim, G.-C. Yi and K. Chang, *Cancer Lett.*, 2010, **299**, 63-71.
199. E. J. Cha, E. S. Jang, I. C. Sun, I. J. Lee, J. H. Ko, Y. I. Kim, I. C. Kwon, K. Kim and C. H. Ahn, *J. Controlled Release*, 2011, **155**, 152-158.
200. D. W. Hwang, H. Y. Ko, J. H. Lee, H. Kang, S. H. Ryu, I. C. Song, D. S. Lee and S. Kim, *J. Nucl. Med.*, 2010, **51**, 98-105.
201. Y. Mi, K. Li, Y. Liu, K.-Y. Pu, B. Liu and S.-S. Feng, *Biomaterials*, 2011, **32**, 8226-8233.
202. J.-H. Lee, Y.-W. Jun, S.-I. Yeon, J.-S. Shin and J. Cheon, *Angew. Chem. Int. Ed.*, 2006, **45**, 8160-8162.
203. S. S. Kelkar and T. M. Reineke, *Bioconj. Chem.*, 2011, **22**, 1879-1903.
204. P. K. Jain, X. Huang, I. H. El-Sayed and M. A. El-Sayed, *Acc. Chem. Res.*, 2008, **41**, 1578-1586.
205. H.-L. Tu, Y.-S. Lin, H.-Y. Lin, Y. Hung, L.-W. Lo, Y.-F. Chen and C.-Y. Mou, *Adv. Mater.*, 2009, **21**, 172-177.
206. H. Maeda, J. Wu, T. Sawa, Y. Matsumura and K. Hori, *J. Controlled Release*, 2000, **65**, 271-284.
207. I. M. Rio-Echevarria, F. Selvestrel, D. Segat, G. Guarino, R. Tavano, V. Causin, E. Reddi, E. Papini and F. Mancin, *J. Mater. Chem.*, 2010, **20**, 2780-2787.
208. X. He, X. Wu, K. Wang, B. Shi and L. Hai, *Biomaterials*, 2009, **30**, 5601-5609.
209. X. F. Qiao, J. C. Zhou, J. W. Xiao, Y. F. Wang, L. D. Sun and C. H. Yan, *Nanoscale*, 2012, **4**, 4611-4623.
210. A. M. Fales, H. Yuan and T. Vo-Dinh, *Langmuir*, 2011, **27**, 12186-12190.
211. F. Wang, X. Chen, Z. Zhao, S. Tang, X. Huang, C. Lin, C. Cai and N. Zheng, *J. Mater. Chem.*, 2011, **21**, 11244-11252.
212. S.-H. Cheng, C.-H. Lee, M.-C. Chen, J. S. Souris, F.-G. Tseng, C.-S. Yang, C.-Y. Mou, C.-T. Chen and L.-W. Lo, *J. Mater. Chem.*, 2010, **20**, 6149-6157.
213. J. Yu, M. A. Yaseen, B. Anvari and M. S. Wong, *Chem. Mater.*, 2007, **19**, 1277-1284.
214. A. M. Schwartzberg and J. Z. Zhang, *J. Phys. Chem. C*, 2008, **112**, 10323-10337.
215. J. Z. Zhang, *J. Phys. Chem. Lett.*, 2010, **1**, 686-695.
216. G. Battistini, P. G. Cozzi, J.-P. Jalkanen, M. Montalti, L. Prodi, N. Zaccheroni and F. Zerbetto, *ACS Nano*, 2007, **2**, 77-84.
217. P. Sharma, S. C. Brown, A. Singh, N. Iwakuma, G. Pyrgiotakis, V. Krishna, J. A. Knapik, K. Barr, B. M. Moudgil and S. R. Grobmyer, *J. Mater. Chem.*, 2010, **20**, 5182-5185.
218. A. K. Singh, M. A. Hahn, L. G. Gutwein, M. C. Rule, J. A. Knapik, B. M. Moudgil, S. R. Grobmyer and S. C. Brown, *Int. J. Nanomed.*, 2012, **7**, 2739-2750.
219. Y. Chen, Q. Yin, X. Ji, S. Zhang, H. Chen, Y. Zheng, Y. Sun, H. Qu, Z. Wang, Y. Li, X. Wang, K. Zhang, L. Zhang and J. Shi, *Biomaterials*, 2012, **33**, 7126-7137.
220. J. Wan, X. Meng, E. Liu and K. Chen, *Nanotechnology*, 2010, **21**, 235104/235101-235104/235108, S235104/235101.
221. Y. Li and W. Xu, *New Microbiol.*, 2009, **32**, 377-383.
222. K. L. Ai, B. H. Zhang and L. H. Lu, *Angew. Chem. Int. Ed.*, 2009, **48**, 304-308.
223. Z. Wang, T. Miu, H. Xu, N. Duan, X. Ding and S. Li, *J. Microbiol. Methods*, 2010, **83**, 179-184.
224. A. Ekrami, A. R. Samarbaf-Zadeh, A. Khosravi, B. Zargar, M. Alavi, M. Amin and A. Kiasat, *Int. J. Nanomed.*, 2011, **6**, 2729-2735.
225. C. Song, Z. Ye, G. Wang, D. Jin, J. Yuan, Y. Guan and J. Piper, *Talanta*, 2009, **79**, 103-108.
226. S. Zanarini, E. Rampazzo, L. Della Ciana, M. Marcaccio, E. Marzocchi, M. Montalti, F. Paolucci and L. Prodi, *J. Am. Chem. Soc.*, 2009, **131**, 2260-2267.
227. L. M. Bronstein and Z. B. Shifrina, *Chem. Rev.*, 2011, **111**, 5301-5344.
228. V. Gubala, X. Le Guevel, R. Nooney, D. E. Williams and B. MacCraith, *Talanta*, 2010, **81**, 1833-1839.
229. R. Woolley, S. Roy, U. Prendergast, A. Panzera, L. Basabe-Desmonts, D. Kenny and C. McDonagh, *Nanomed. Nanotechnol.*, 2013, **9**, 540-549.
230. R. Ricco, A. Meneghello and F. Enrichi, *Biosensors Bioelectron.*, 2011, **26**, 2761-2765.
231. H.-M. Liu, S.-H. Wu, C.-W. Lu, M. Yao, J.-K. Hsiao, Y. Hung, Y.-S. Lin, C.-Y. Mou, C.-S. Yang, D.-M. Huang and Y.-C. Chen, *Small*, 2008, **4**, 619-626.
232. T. H. Kim, J. K. Kim, W. Shim, S. Y. Kim, T. J. Park and J. Y. Jung, *Magn. Reson. Imaging*, 2010, **28**, 1004-1013.
233. S.-H. Wu, Y.-S. Lin, Y. Hung, Y.-H. Chou, Y.-H. Hsu, C. Chang and C.-Y. Mou, *ChemBioChem*, 2008, **9**, 53-57.
234. E. L. Que, D. W. Domaille and C. J. Chang, *Chem. Rev.*, 2008, **108**, 1517-1549.
235. L. Prodi, *New J. Chem.*, 2005, **29**, 20-31.
236. S. Bonacchi, D. Genovese, R. Juris, M. Montalti, L. Prodi, E. Rampazzo, M. Sgarzi and N. Zaccheroni, *Top. Curr. Chem.*, 2011, **300**, 93-138
237. C. Lodeiro, J. L. Capelo, J. C. Mejuto, E. Oliveira, H. M. Santos, B. Pedras and C. Nunez, *Chem. Soc. Rev.*, 2010, **39**, 2948-2976.
238. Y. Qin, J. G. Miranda, C. I. Stoddard, K. M. Dean, D. F. Galati and A. E. Palmer, *ACS Chem. Biol.*, 2013.
239. S. Zhu, T. Fisher, W. Wan, A. B. Descalzo and K. Rurack, *Top. Curr. Chem.*, 2011, **300**, 51-92.
240. L. Bau, P. Tecilla and F. Mancin, *Nanoscale*, 2011, **3**, 121-133.
241. A. Burns, H. Ow and U. Wiesner, *Chemical Society Reviews*, 2006, **35**, 1028-1042.
242. L. Wang, K. M. Wang, S. Santra, X. J. Zhao, L. R. Hilliard, J. E. Smith, J. R. Wu and W. H. Tan, *Anal. Chem.*, 2006, **78**, 646-654.
243. V. Sokolova and M. Epple, *Nanoscale*, 2011, **3**, 1957-1962.
244. A. Schulz and C. McDonagh, *Soft Matter*, 2012, **8**, 2579-2585.
245. M. Schaferling, *Angew. Chem. Int. Ed.*, 2012, **51**, 3532-3554.
246. J. H. Jung, J. H. Lee and S. Shinkai, *Chem. Soc. Rev.*, 2011, **40**, 4464-4474.
247. M. Montalti, L. Prodi and N. Zaccheroni, *J. Mater. Chem.*, 2005, **15**, 2810-2814.

248. E. Rampazzo, E. Brasola, S. Marcuz, F. Mancin, P. Tecilla and U. Tonellato, *J. Mater. Chem.*, 2005, **15**, 2687-2696.
249. E. Brasola, F. Mancin, E. Rampazzo, P. Tecilla and U. Tonellato, *Chem. Commun.*, 2003, 3026-3027.
250. P. Teolato, E. Rampazzo, M. Arduini, F. Mancin, P. Tecilla and U. Tonellato, *Chemistry – A European Journal*, 2007, **13**, 2238-2245.
251. S. Bonacchi, E. Rampazzo, M. Montalti, L. Prodi, N. Zaccheroni, F. Mancin and P. Teolato, *Langmuir*, 2008, **24**, 8387-8392.
252. L. Zeng, E. W. Miller, A. Pralle, E. Y. Isacoff and C. J. Chang, *J. Am. Chem. Soc.*, 2005, **128**, 10-11.
253. E. Oliveira, D. Genovese, R. Juris, N. Zaccheroni, J. L. Capelo, M. M. M. Raposo, S. P. G. Costa, L. Prodi and C. Lodeiro, *Inorg. Chem.*, 2011, **50**, 8834-8849.
254. C. Bazzicalupi, C. Caltagirone, Z. Cao, Q. Chen, C. Di Natale, A. Garau, V. Lippolis, L. Lvova, H. Liu, I. Lundström, M. C. Mostallino, M. Nieddu, R. Paolesse, L. Prodi, M. Sgarzi and N. Zaccheroni, *Chemistry – A European Journal*, 2013, **19**, 14639-14653.
255. L. Baù, F. Selvestrel, M. Arduini, I. Zamparo, C. Lodovichi and F. Mancin, *Org. Lett.*, 2012, **14**, 2984-2987.
256. D. Cauzzi, R. Pattacini, M. Delferro, F. Dini, C. Di Natale, R. Paolesse, S. Bonacchi, M. Montalti, N. Zaccheroni, M. Calvaresi, F. Zerbetto and L. Prodi, *Angew. Chem. Int. Ed.*, 2012, **51**, 9662-9665.

 